

Provable non-convex projected gradient descent for a class of constrained matrix optimization problems

Dohyung Park¹, Anastasios Kyrillidis¹, Srinadh Bhojanapalli²
Constantine Caramanis¹, and Sujay Sanghavi¹

¹The University of Texas at Austin
 {dhpark, anastasios, constantine}@utexas.edu,
 sanghavi@mail.utexas.edu

²Toyota Technological Institute at Chicago
 srinadh@ttic.edu

July 29, 2022

Abstract

We propose a simple and scalable non-convex method for low-rank PSD matrix problems with a generic (strongly) convex objective f , and additional matrix norm constraints. Such criteria appear in quantum state tomography and phase retrieval applications, among others. However, without careful design, existing methods quickly run into time and memory bottlenecks, as problem dimensions increase.

To remedy these shortcomings, we propose the *Projected Factored Gradient Descent* (ProjFGD) algorithm, that operates on the *low-rank factorization* of the variable space. Such factorization imputes non-convexity in the optimization; nevertheless, we show that our method favors local linear convergence rate in the non-convex factored space, for a class of convex norm-constrained problems. We build our theory on a novel *descent lemma*, that extends recent results on the unconstrained version of the problem. Our findings are supported by empirical evidence on quantum state tomography and sparse phase retrieval applications.

1 Introduction

We consider matrix optimization problems that can be expressed as:

$$\underset{X \in \mathbb{R}^{n \times n}}{\text{minimize}} \quad f(X) \quad \text{subject to} \quad X \succeq 0, \quad X \in \mathcal{C}'. \quad (1)$$

Here, f is assumed to be strongly convex and Lipschitz gradient continuous. Moreover, let the optimum X^* of (1) satisfy $\text{rank}(X^*) = r^*$, where $r^* \leq n$, and let $\mathcal{C}' \subseteq \mathbb{R}^{n \times n}$ denote additional, convex constraints on X . Observe that (1) is convex, under these assumptions. Nevertheless, in practice we usually force the estimate to be low-rank (even if $r^* = n$) –e.g., due to statistical or computational reasons— in order to hope for a good approximation of X^* in reasonable time; in such cases, the problem becomes non-convex. We will focus on such low-rank cases where (i) either X^* is low-rank by nature, (ii) or we are interested in estimating a low-rank approximation of X^* .

Such criteria appear naturally (or at least after simple transformations) in applications from diverse research fields; a non-exhaustive list includes density matrix estimation of quantum systems (where \mathcal{C}' includes trace norm constraints on X) [1, 23, 29], sparse phase retrieval applications such as X-ray crystallography and microscopy [26, 42, 38], and sparse PCA [31] (where \mathcal{C}' contains ℓ_1 -norm constraints

on X); see Section 4 for more details. In all cases, the number of variables grows fast, as the problem dimensions increase. Thus, due to their widespread occurrence, it is critical to devise easy-to-implement, efficient and provable algorithms.

For specific instances of (1), researchers have devised such algorithms that solve (1), even when non-convex rank constraints are present; even a brief overview of the techniques used would go beyond the page limits of this paper. As representative algorithmic realizations, we mention [27, 7, 4, 9, 45, 32, 30, 28, 43, 24, 47] and point to references therein: most of these schemes, though, focus on the matrix sensing / matrix completion problem, and, thus, are designed for specific instances of f . Moreover, the majority of them do not directly handle additional constraints.

To even a greater extent, there is ample discussion on how to solve rank-constrained instances of (1) in the *convex* setting, where the rank constraint is substituted by the nuclear norm of X ; we refer the reader to [34, 6, 13, 5, 17, 46] and references therein for useful pointers.

Nevertheless, these methods often involve top- r singular value/vector computations –at least once per iteration– in order to hope for good approximate solution, due to rank/nuclear norm constraints (especially in under-determined problem cases). This constitutes their computational bottleneck in large-scale settings. Thus, it is desirable to find algorithms that scale well in practice.

Our approach. One way to achieve this is by *low-rank matrix factorization* techniques. In particular, we solve instances of (1) in the factored form as follows:

$$\underset{U \in \mathbb{R}^{n \times r}}{\text{minimize}} \quad f(UU^\top) \quad \text{subject to} \quad U \in \mathcal{C}. \quad (2)$$

This formulation, popularized by Burer and Monteiro [11, 12], naturally encodes the PSD constraint in (2), removing the expensive eigen-decomposition projection step. Here, $r \leq r^*$ is often set to be much smaller than r^* , due to statistical or computational reasons, as mentioned above; thus, by construction, the UU^\top matrix is *low-rank* and PSD.

$\mathcal{C} \subseteq \mathbb{R}^{n \times r}$ is a compact convex set, that models well \mathcal{C}' in (1). While in practice we can assume any such constraint \mathcal{C} with *tractable* Euclidean projection operator¹, in our theory we mostly focus on *norm constraint sets* for \mathcal{C} . As we describe next in more detail, in order to claim convergence to a useful estimate in the X space through the factored U space, we require \mathcal{C} and \mathcal{C}' be connected via a continuous map $U \mapsto X$, such that any point U in \mathcal{C} has a representative point $X = UU^\top$ in \mathcal{C}' . We defer this discussion to Section 3.

Our motivation for studying (2) origins from large-scale problem instances: when r is much smaller than n , factor $U \in \mathbb{R}^{n \times r}$ contains much less variables to maintain and optimize than $X = UU^\top$. Thus, by construction, such parametrization also makes it easier to update and store the iterates U . Even more importantly, observe that UU^\top reformulation automatically encodes any rank constraint. Standard approaches, that operate in the original variable space, either enforce such constraint at every iteration or involve a nuclear-norm projection. Doing so requires computing a truncated SVD per iteration, which can get cumbersome in large-scale settings.

Contributions. Our aim is to broaden the results on efficient, non-convex recovery for *constrained* low-rank matrix problems. In order to have a more user-friendly theory and algorithm, our developments maintain a connection with analogous results in convex optimization, where standard assumptions are made. To this end, we extend the results in [8] (see Section 1.1 for a more complete discussion on related work), and consider the common case where f is smooth and (restricted) strongly convex [2]; extension to just smooth f cases is left for future work.² From a practical point of view, we provide

¹In general, one could artificially introduce \mathcal{C} in (2), even when no \mathcal{C}' constraint is present in (1) (e.g., for better interpretation of results).

²We consider here the strongly convex case since such cases are usually more interesting in practice, as we show in the experiments section.

experimental results for two important tasks in physical sciences: quantum state density estimation and sparse phase retrieval.

Some highlights of our developments are the following:

- A key property for proving convergence in convex optimization, under common smoothness and strong convexity assumptions, is the notion of *descent*. *I.e.*, given current, next and optimal points in the X space, say X_t, X_{t+1}, X^* , respectively, and the recursion $X_{t+1} = X_t - \eta \nabla f(X_t)$, the condition $\langle X_t - X_{t+1}, X_t - X^* \rangle \geq C$ –where $C > 0$ depends on the gradient norm– implies that X_{t+1} “moves” towards the correct direction.³ Similar results have been proved in [8] on the non-convex factored-space, however *without constraints*. In this work, we present a *novel descent lemma* that non-trivially extends such conditions for (2), for a simple case of norm-based convex sets \mathcal{C} . We hope that this result will trigger more attempts towards more generic convex sets.
- We propose **ProjFGD**, a non-convex projected gradient descent algorithm that solves instances of (2). **ProjFGD** has a novel constant step size selection procedure, following ideas from [8], that leads to favorable local convergence guarantees when f is smooth and (restricted) strongly convex. We also present an initialization procedure with some guarantees in the supplementary material.
- Finally, we extensively study the performance of **ProjFGD** on two problem cases: (i) quantum state tomography and (ii) sparse phase retrieval. Our findings show significant acceleration when **ProjFGD** is used, as compared to state of the art.

1.1 Related work

Here, we elaborate a bit further on an evolving line of work that considers problem variants of (2), where factorizations of the form UU^\top are used.

The work of [18] proposes a first-order algorithm for (2), where the nature of the constraint set is more generic than the one we consider here, and depends on the problem at hand. The authors provided a set of conditions (local descent, local Lipschitz, and local smoothness) under which one can prove convergence to an ε -close solution with $O(1/\varepsilon)$ or $O(\log(1/\varepsilon))$ iterations. While the convergence proof is general, checking whether the three conditions hold is a non-trivial problem and requires different analysis depending on a particular estimation problem at hand.

[8] proposes the *Factored Gradient Descent* (FGD) algorithm for (2), where $\mathcal{C} \equiv \mathbb{R}^{n \times r}$. FGD is also a first-order scheme. Key ingredient for convergence is a novel step size selection that can be used for any f , as long as it is Lipschitz gradient smooth (and strongly convex for faster convergence). However, [8] cannot accommodate any constraints on U . Notwithstanding this limitation, [8] is the first paper that *provably* solves the unconstrained re-parametrized problem in (2) for generic convex functions f , under *common convex assumptions*.

Concurrently, [48] presents a new analysis that handles non-square cases in (2). In that case, we look for a factorization $X = UV^\top \in \mathbb{R}^{n \times p}$. The idea is based on the inexact first-order oracle, previously used in [3]. Similarly to [8], the proposed theory does not handle any constraints and restricts to the case of strongly convex and smooth convex f .

Roadmap. Section 2 contains some basic definitions and assumptions that are repeatedly used in the main text. Section 3 describes **ProjFGD** and its theoretical guarantees. In Section 4, we motivate the necessity of **ProjFGD** via some applications; due to space limitations, only one application is described in the main text (the second application is included in the supplementary material). This paper concludes with a discussion on future directions in Section 5. Supplementary material contains further experiments, all proofs of theorems in main text, and a proposed initialization procedure.

³To see this, observe that $X^* - X_t$ is the best possible direction to follow, while $X_t - X_{t+1}$ is the direction we actually follow. Then, such a condition implies that there is a non-trivial positive correlation between these two directions.

2 Preliminaries

Notation. For matrices $X, Y \in \mathbb{R}^{n \times n}$, $\langle X, Y \rangle = \text{Tr}(X^\top Y)$ represents their inner product. $X \succeq 0$ denotes X is a positive semi-definite (PSD) matrix. We use $\|X\|_F$ and $\sigma_1(X)$ for the Frobenius and spectral norms of a matrix, respectively; we also use $\|X\|_2$ to denote the spectral norm. Moreover, we denote as $\sigma_i(X)$ the i -th singular value of X . X_r denotes the best rank- r approximation of X . For X such that $X = UU^\top$, the gradient of f with respect to U is $(\nabla f(UU^\top) + \nabla f(UU^\top)^\top)U$. If f is also symmetric, *i.e.*, $f(X) = f(X^\top)$, then $\nabla f(X) = 2\nabla f(X) \cdot U$.

An important issue in optimizing f over the factored space is the existence of non-unique possible factorizations. We use the following rotation invariant distance metric:

Definition 2.1. Let matrices $U, V \in \mathbb{R}^{n \times r}$. Define:

$$\text{DIST}(U, V) := \min_{R: R \in \mathcal{O}} \|U - VR\|_F, \quad \text{where } \mathcal{O} \text{ is the set of } r \times r \text{ orthonormal matrices } R.$$

Assumptions. We consider applications that can be described by *strongly* convex functions f with *gradient Lipschitz continuity*.⁴ We state these standard definitions below for the square case.

Definition 2.2. Let $f: \mathbb{R}^{n \times n} \rightarrow \mathbb{R}$ be convex and differentiable. Then, f is μ -strongly convex if:

$$f(Y) \geq f(X) + \langle \nabla f(X), Y - X \rangle + \frac{\mu}{2} \|Y - X\|_F^2, \quad \forall X, Y \in \mathbb{R}^{n \times n}. \quad (3)$$

Definition 2.3. Let $f: \mathbb{R}^{n \times p} \rightarrow \mathbb{R}$ be a convex differentiable function. Then, f is gradient Lipschitz continuous with parameter L (or L -smooth) if:

$$\|\nabla f(X) - \nabla f(Y)\|_F \leq L \cdot \|X - Y\|_F, \quad \forall X, Y \in \mathbb{R}^{n \times n}. \quad (4)$$

For our proofs, we will also make the *faithfulness* assumption, as in [18]:

Definition 2.4. Let \mathcal{E} denote the set of equivalent factorizations that lead to a rank- r matrix $X^* \in \mathbb{R}^{n \times n}$; *i.e.*, $\mathcal{E} := \{U^* \in \mathbb{R}^{n \times r} : X^* = U^*U^{*\top}\}$. Then, we assume $\mathcal{E} \subseteq \mathcal{C}$, *i.e.*, the resulting convex set \mathcal{C} in (2) (from \mathcal{C}' in (1)) respects the structure of \mathcal{E} .

This assumption is necessary for arguments regarding the quality of solution obtained in the factored U space, w.r.t. the original X space.

3 The Projected Factored Gradient Descent (ProjFGD) algorithm

Let us first describe the ProjFGD algorithm, a projected, first-order scheme. The pseudocode is provided in Algorithm 1. Let $\Pi_{\mathcal{C}}(V)$ denote the projection of an input matrix $V \in \mathbb{R}^{n \times r}$ onto the convex set \mathcal{C} . The starting point is then computed as follows: we first compute $X_0 := 1/\hat{L} \cdot \Pi_+(-\nabla f(0))$, where $\Pi_+(\cdot)$ denotes the projection onto the set of PSD matrices and \hat{L} represents an approximation of L ; see also [8]. Then, ProjFGD requires a top- r SVD calculation, *only once*, to compute $\tilde{U}_0 \in \mathbb{R}^{n \times r}$, such that $X_0 = \tilde{U}_0 \tilde{U}_0^\top$; using \tilde{U}_0 , the initial point U_0 satisfies $U_0 = \Pi_{\mathcal{C}}(\tilde{U}_0)$, in order to accommodate constraints \mathcal{C} .

The main iteration of ProjFGD applies the simple rule for any iteration t :

$$U_{t+1} = \Pi_{\mathcal{C}} \left(U_t - \eta \nabla f(U_t U_t^\top) \cdot U_t \right),$$

⁴Our ideas can be extended in a similar fashion to the case of restricted strong convexity [2].

Algorithm 1 ProjFGD method

input Function f , target rank r , # iterations T .

- 1: Compute $X_0 := 1/\hat{L} \cdot \Pi_+(-\nabla f(0))$.
- 2: Set $\tilde{U}_0 \in \mathbb{R}^{n \times r}$ such that $X_0 = \tilde{U}_0 \tilde{U}_0^\top$.
- 3: Compute $U_0 = \Pi_{\mathcal{C}}(\tilde{U}_0)$.
- 4: Set step size η as in (5).
- 5: **for** $t = 0$ to $T - 1$ **do**
- 6: $U_{t+1} = \Pi_{\mathcal{C}}(U_t - \eta \nabla f(U_t U_t^\top) \cdot U_t)$.
- 7: **end for**

output $X = U_T U_T^\top$.

with step size:

$$\eta \leq \frac{1}{128(L\|X_0\|_2 + \|\nabla f(X_0)\|_2)}. \quad (5)$$

Here, one can use \hat{L} to approximate L .

Key ingredients to achieve provable convergence are the initialization step –so that initial point U_0 leads to $\text{DIST}(U_0, U^*)$ sufficiently small– and the step size selection. For the initialization, apart from the procedure mentioned above, we could also use more specialized spectral methods –see [18, 49]– or even run algorithms, applied on the original variable space (1), for only a few iterations –this requires further full or truncated SVDs [44]. The discussion regarding our initialization and what type of guarantees one obtains is deferred to the supplementary material.

To retain the computational efficiency per iteration, one might consider constrained problems where the convex set \mathcal{C} is endowed with a *tractable* Euclidean projection operation⁵; however, this assumption does not affect any theoretical guarantees of ProjFGD.

3.1 When constrained non-convex problems can be scary?

In stark contrast to the *convex* projected gradient descent method, proving convergence guarantees for (2) is not a straightforward task. First, if we are interested in quantifying the quality of the solution in the factored space w.r.t. X^* , \mathcal{C} should be *faithful*, according to Definition 2.1. Furthermore, there should exist a continuous map $U \mapsto X$ that relates the constraint set \mathcal{C}' , in the original variable space (see (1)), to the factored one \mathcal{C} (see (2)). In that case, claims about convergence to a point U^* , in the factored space, can be “transformed” into claims about convergence to a point close to X^* , in the original space. As an example, consider the case where, for any $X = UU^\top$, $\text{TR}(X) \leq \lambda \Leftrightarrow \|U\|_F^2 \leq \lambda$, and, thus, satisfying $\|U\|_F^2 \leq \lambda$, for any U , guarantees that $\text{TR}(X) \leq \lambda$ for $X = UU^\top$. Apart from the example above, other characteristic cases include Schatten norms.

Contrary to this example, consider the case $\mathcal{C}' := \{X \in \mathbb{R}^{n \times n} : \|X\|_1 \leq \lambda'\}$, where, $\|X\|_1 = \sum_{ij} |X_{ij}|$. A natural choice for \mathcal{C} would be $\mathcal{C} := \{U \in \mathbb{R}^{n \times r} : \|U\|_1 \leq \lambda\}$, for $\lambda, \lambda' > 0$; however, depending on the selection of λ , w.r.t. λ' , points in $U \in \mathcal{C}$ might result into points in the original space $X = UU^\top$ that $X \notin \mathcal{C}'$. In this case, U^* of (2) could be $U^* \notin \mathcal{E}$ and, thus, convergence guarantees to U^* have no meaning in convergence in X space. However, as we show in Section 6.1, in this case \mathcal{C} “simulates” fairly well \mathcal{C}' in the original space: if U is sparse enough, then $X = UU^\top$ could also be fairly sparse, so proper selection of λ plays a key role. Even in this case, ProjFGD still performs competitively compared to state-of-the-art approaches.

Second, the projection step itself complicates considerably the analysis due to non-convexity, as we show in the supplementary material. In our theory, we focus on convex sets \mathcal{C} that satisfy (6)

⁵If the projection predominates the per iteration complexity, such that an top- r SVD calculation has comparable complexity, then one might consider operating on the original X variable space.

where $\Pi_{\mathcal{C}}(V)$ can be equivalently seen as scaling the input. *E.g.*, when $\mathcal{C} \equiv \{U \in \mathbb{R}^{n \times r} : \|U\|_F \leq \lambda\}$, $\Pi_{\mathcal{C}}(V) = \xi(V) \cdot V$ where $\xi(V) := \frac{\lambda}{\|V\|_F}$, for $V \notin \mathcal{C}$. Our theory highlights that, even for this simple case, proving convergence is not a straightforward task.

3.2 Theoretical guarantees of ProjFGD for $\mathcal{C} := \{U \in \mathbb{R}^{m \times r} : \|U\|_F \leq \lambda\}$

We provide theoretical guarantees for ProjFGD in the case where the constraint satisfies

$$\Pi_{\mathcal{C}}(V) = \operatorname{argmin}_{U \in \mathcal{C}} \frac{1}{2} \|U - V\|_F^2 = \begin{cases} V & \text{if } V \in \mathcal{C}, \\ \xi(V) \cdot V & \text{if } V \notin \mathcal{C}, \end{cases} \quad (6)$$

i.e., the projection operation is an *entry-wise scaling*. Such settings include the Frobenius norm constraint $\mathcal{C} = \{U \in \mathbb{R}^{m \times r} : \|U\|_F \leq \lambda\}$, which appears in quantum state tomography. Moreover, for this case, the constraint has one-to-one correspondence with the trace constraint in the original X space; thus any argument in the U space applies for the X space also.

We assume the optimum X^* satisfies $\operatorname{rank}(X^*) = r^*$. To solve (1), we optimize over the re-parameterized problem (2), with the *faithful* constraint set \mathcal{C} satisfying the properties above.

For our analysis, we will use the following step sizes:

$$\hat{\eta} = \frac{1}{128(L\|X_t\|_2 + \|Q_{U_t} Q_{U_t}^\top \nabla f(X_t)\|_2)}, \quad \eta^* = \frac{1}{128(L\|X^*\|_2 + \|\nabla f(X^*)\|_2)},$$

where Q_A is a basis for column space of A . By Lemma A.5 in [8], we know that $\hat{\eta} \geq \frac{5}{6}\eta$ and $\frac{10}{11}\eta^* \leq \eta \leq \frac{11}{10}\eta^*$. Due to such relationships, in our proof we will work with step size $\hat{\eta}$: this is equivalent –up to constants– to the original step size η , used in the algorithm. Thus, any results below will automatically imply similar results hold for η , by using the bounds between step sizes.

Theorem 3.1 ((Local) convergence rate for restricted strongly convex and smooth f). *Let $\mathcal{C} \subseteq \mathbb{R}^{n \times r}$ be a convex, compact, and faithful set, with projection operator satisfying (6). Let $U_t \in \mathcal{C}$ be the current estimate and $X_t = U_t U_t^\top$. Assume current point U_t satisfies $\operatorname{DIST}(U_t, U^*) \leq \rho' \sigma_r(U^*)$, for $\rho' := c \cdot \frac{\mu}{L} \cdot \frac{\sigma_r(X^*)}{\sigma_1(X^*)}$, $c \leq \frac{1}{200}$, and given $\xi_t(\cdot) \gtrsim 0.78$ per iteration, the new estimate of ProjFGD, $U_{t+1} = \Pi_{\mathcal{C}}(U_t - \hat{\eta} \nabla f(U_t U_t^\top) \cdot U_t) = \xi_t \cdot (U_t - \hat{\eta} \nabla f(U_t U_t^\top) \cdot U_t)$ satisfies*

$$\operatorname{DIST}(U_{t+1}, U^*)^2 \leq \alpha \cdot \operatorname{DIST}(U_t, U^*)^2, \quad (7)$$

where $\alpha := 1 - \frac{\mu \cdot \sigma_r(X^*)}{550(L\|X^*\|_2 + \|\nabla f(X^*)\|_2)} < 1$. Further, U_{t+1} satisfies $\operatorname{DIST}(U_{t+1}, U^*) \leq \rho' \sigma_r(U^*)$.

The complete proof of the theorem is provided in the supplementary material. The assumption $\operatorname{DIST}(U_t, U^*) \leq \rho' \sigma_r(U^*)$ only leads to a local convergence result. [18] provide some initialization procedures for different applications, where we can find an initial point U_0 such that $\operatorname{DIST}(U_0, U^*) \leq \rho' \sigma_r(U^*)$ is satisfied. In the supplementary material, we present a similar generic initialization procedure that results in exact recovery of the optimum, under further assumptions. We borrow such procedure in Section 4 for our experiments.

$\xi_t(\cdot)$ requirement. The assumption $\xi_t(\cdot) \gtrsim 0.78$ implies the iterates of ProjFGD (before the projection step) are retained relatively close to the set \mathcal{C} .⁶ For some cases, this can be easily satisfied by setting the step size small enough, as indicated below; the proof can be found in Section 7.

Corollary 3.2. *If $\mathcal{C} = \{U \in \mathbb{R}^{n \times r} : \|U\|_F \leq \lambda\}$, then ProjFGD inherently satisfies $\frac{128}{129} \leq \xi_t(\cdot) \leq 1$, for every t . *I.e.*, it guarantees (7) without assumptions on $\xi_t(\cdot)$.*

⁶Intuitively, we expect the estimates U_t , before the projection, to be further from \mathcal{C} during the first steps of ProjFGD; as the number of iterations increases, the sequence of solutions gets closer to U^* and thus $\xi_t(\cdot) \rightarrow 1$.

We conjecture that the lower bound on $\xi_t(\cdot)$ could possibly be improved with a different analysis.

Key lemma. The proof of the above theorem primarily depends on the following “descent” lemma for ProjFGD.

Lemma 3.3 (Descent lemma). *Let $\tilde{U}_{t+1} = U_t - \hat{\eta} \nabla f(X_t^\top) \cdot U_t$. For f L -smooth and μ -strongly convex, and under the same assumptions with Theorem 3.1, the following inequality holds true:*

$$2\hat{\eta} \langle \nabla f(U_t U_t^\top) \cdot U_t, U_t - U^* R_{U_t}^* \rangle + \|U_{t+1} - \tilde{U}_{t+1}\|_F^2 \geq \hat{\eta}^2 \|\nabla f(U_t U_t^\top) U_t\|_F^2 + \frac{3\hat{\eta}\mu}{10} \cdot \sigma_r(X^*) \cdot \text{DIST}(U_t, U^*)^2.$$

In the unconstrained case, [8] proposes a similar bound (Lemma 6.1 in [8]):

$$2\hat{\eta} \langle \nabla f(U_t U_t^\top) \cdot U_t, U_t - U^* R_{U_t}^* \rangle \geq \frac{4\hat{\eta}^2}{3} \|\nabla f(U_t U_t^\top) U_t\|_F^2 + \frac{3\hat{\eta}\mu}{20} \cdot \sigma_r(X^*) \cdot \text{DIST}(U_t, U^*)^2. \quad (8)$$

However, their result and its analysis does not directly apply in our case: their techniques are oblivious of any convex constraints on the X -space (or the U -space).⁷

4 Applications

We present two characteristic applications. For each application, we define the problem, enumerate state-of-the-art algorithms and provide numerical results. We refer the reader to Section 6 for additional experiments.

4.1 Quantum state tomography

Building on Aaronson’s work on quantum state tomography (QST) [1], we are interested in learning the (almost) *pure*⁸ q -bit state of a quantum system –known as the density matrix– via a limited set of measurements. In math terms, the problem can be cast as follows. Let us define the *density matrix* $X^* \in \mathbb{C}^{n \times n}$ of a q -bit quantum system as an unknown Hermitian, positive semi-definite matrix that satisfies $\text{rank}(X^*) = r$ and is normalized as $\text{TR}(X^*) = 1$ [23]; here, $n = 2^q$. Our task is to recover X^* from a set of QST measurements $y \in \mathbb{R}^m$, $m \ll n^2$, that satisfy $y = \mathcal{A}(X^*) + \eta$. Here, $(\mathcal{A}(X^*))_i = \text{TR}(E_i X^*)$ and η_i can be modeled as independent, zero-mean normal variables. The operators $E_i \in \mathbb{R}^{n \times n}$ are typically the tensor product of the 2×2 Pauli matrices⁹ [35].

The above lead to the following *non-convex* problem formulation¹⁰:

$$\underset{X \succeq 0}{\text{minimize}} \quad \|\mathcal{A}(X) - y\|_F^2 \quad \text{subject to} \quad \text{rank}(X) = r, \text{TR}(X) \leq 1. \quad (10)$$

⁷To see this, in the unconstrained case, if $U_t \equiv U^*$ (up to some rotation), then the following holds

$$0 := 2\hat{\eta} \langle \nabla f(X^*) \cdot U^*, U^* - U^* R_{U_t}^* \rangle \geq \frac{4\hat{\eta}^2}{3} \|\nabla f(X^*) U^*\|_F^2 + \frac{3\hat{\eta}\mu}{20} \cdot \sigma_r(X^*) \cdot \text{DIST}(U^*, U^*)^2 =: 0,$$

since at the optimum we have $\nabla f(X^*) U^* = 0$. Though, given constraints, such condition does not hold in (8).

⁸Purity is a structural property of the density matrix: A quantum systems is *pure* if its density matrix is rank one and, *almost pure* if it can be well-approximated by a low rank matrix.

⁹[35] showed that, for almost all such tensor constructions –of $m = O(rn \log^c n)$, $c > 0$, Pauli measurements– satisfy the so-called rank- r restricted isometry property (RIP) for all $X \in \{X : X \succeq 0, \text{rank}(X) \leq r, \|X\|_* \leq \sqrt{r} \|X\|_F\}$:

$$(1 - \delta_r) \|X\|_F^2 \leq \|\mathcal{A}(X)\|_F^2 \leq (1 + \delta_r) \|X\|_F^2, \quad (9)$$

where $\|\cdot\|_*$ is the nuclear norm (i.e., the sum of singular values), which reduces to $\text{TR}(X)$ since $X \succeq 0$.

¹⁰As pointed out in [29], it is in fact advantageous in practice to choose $\text{TR}(X) \neq 1$, as it improves the robustness to noise. Here, we force $\text{TR}(X) \leq 1$.

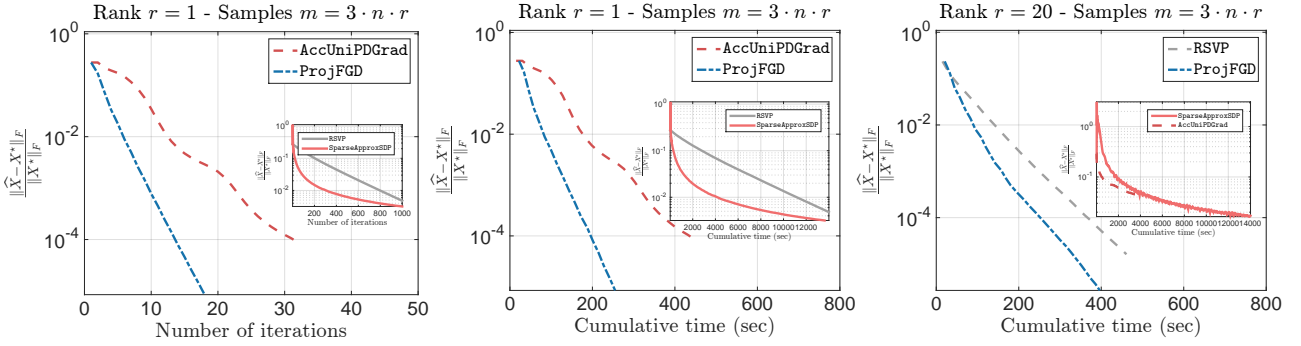


Figure 1: **Left and middle panels:** Convergence performance of algorithms under comparison w.r.t. $\frac{\|\hat{X} - X^*\|_F}{\|X^*\|_F}$ vs. (i) the total number of iterations (left) and (ii) the total execution time. Both cases correspond to $C_{\text{sam}} = 3$, $r = 1$ (pure setting) and $q = 12$ (i.e., $n = 4096$). **Right panel:** Almost pure state ($r = 20$). Here, $C_{\text{sam}} = 3$.

State-of-the-art approaches. One of the first provable algorithmic solutions for the QST problem was through convexification [40]: this includes nuclear norm minimization approaches [23], as well as proximal variants, as follows:

$$\underset{X \succeq 0}{\text{minimize}} \quad \|\mathcal{A}(X) - y\|_F^2 + \lambda \|X\|_*. \quad (11)$$

Here, $\|\cdot\|_*$ reduces to $\text{Tr}(X)$ since $X \succeq 0$. This approach is considered in the seminal work [23] and is both tractable and amenable to theoretical analysis. The approach does not include any constraint on X .¹¹ As one of the most recent algorithms, we mention the work of [46] where a universal primal-dual convex framework is presented, with the QST problem as application.

From a non-convex perspective, [25] presents **SparseApproxSDP** algorithm that solves (10), when the objective is a generic gradient Lipschitz smooth function. **SparseApproxSDP** solves (10) by updating a putative low-rank solution with rank-1 refinements, coming from the gradient. This way, **SparseApproxSDP** avoids computationally expensive operations per iteration, such as full SVDs. In theory, at the r -th iteration, **SparseApproxSDP** is guaranteed to compute a $\frac{1}{r}$ -approximate solution, with rank at most r , i.e., achieves a sublinear $O(\frac{1}{\varepsilon})$ convergence rate. However, depending on ε , **SparseApproxSDP** might not return a low rank solution. Finally, [7] propose Randomized Singular Value Projection (**RSVP**), a projected gradient descent algorithm for (10), which merges gradient calculations with truncated SVDs via randomized approximations for computational efficiency.

Since the size of these problems grows exponentially with the number of quantum bits, designing fast algorithms that minimize the computational effort required for (10) or (11) is mandatory.

Numerical results. In this case, the factorized version of (10) can be described as:

$$\underset{U \in \mathbb{R}^{n \times r}}{\text{minimize}} \quad \|\mathcal{A}(UU^\top) - y\|_F^2 \quad \text{subject to} \quad \|U\|_F^2 \leq 1. \quad (12)$$

We compare **ProjFGD** with the algorithms described above; as a convex representative implementation, we use the efficient scheme of [46]. We consider two settings: $X^* \in \mathbb{R}^{n \times n}$ is (i) a pure state (i.e., $\text{rank}(X^*) = 1$) and, (ii) an almost pure state (i.e., $\text{rank}(X^*) = r$, for some $r > 1$). For all cases, $\text{Tr}(X^*) = 1$ and $y = \mathcal{A}(X^*)$ (noiseless setting). We use Pauli operators for \mathcal{A} , as described in [35]. The number of measurements m satisfy $m = C_{\text{sam}} \cdot r \cdot n \log(n)$, for various values of C_{sam} .

For all algorithms, we used the correct rank input and trace constraint parameter. All methods that require an SVD routine use `lansvd()` from the PROPACK software package. Experiments and algorithms are implemented on MATLAB environment; we used non-specialized and non-mexified code parts for all

¹¹E.g., in order to take the trace constraint $\text{Tr}(X) = 1$ into account, either λ should be precisely tuned to satisfy this constraint or the final estimator is normalized heuristically to satisfy this constraint [20].

algorithms. For initialization, we use the same starting point for all algorithms, which is either specific (Section 8) or random. We set the tolerance parameter to $\text{tol} := 5 \cdot 10^{-6}$.

Convergence plots. Figure 1 (two-leftmost plots) illustrates the iteration and timing complexities of each algorithm under comparison, for a pure state density recovery setting ($r = 1$). Here, $q = 12$ which corresponds to a $\frac{n(n+1)}{2} = 8,390,656$ dimensional problem; moreover, we assume $C_{\text{sam}} = 3$ and thus the number of measurements are $m = 12,288$. For initialization, we use the proposed initialization in Section 8 for all algorithms: we compute $-\mathcal{A}^*(y)$, extract factor U_0 as the best- r PSD approximation of $-\mathcal{A}^*(y)$, and project U_0 onto \mathcal{C} .

It is apparent that **ProjFGD** converges faster to a vicinity of X^* , compared to the rest of the algorithms; observe also the sublinear rate of **SparseApproxSDP** in the inner plots, as reported in [25].

Figure 2 contains recovery error and execution time results for the case $q = 13$ ($n = 8096$); in this case, we solve a $\frac{n(n+1)}{2} = 33,558,528$ dimensional problem. For this case, **RSVP** and **SparseApproxSDP** algorithms were excluded from the comparison. Appendix provides extensive results, where similar performance is observed for other values of q , C_{sam} .

Figure 1 (rightmost plot) considers the more general case where $r = 20$ (almost pure state density) and $q = 12$. In this case, $m = 245,760$ for $C_{\text{sam}} = 3$. As r increases, algorithms that utilize an SVD routine spend more CPU time on singular value/vector calculations. Certainly, the same applies for matrix-matrix multiplications; however, in the latter case, the complexity scale is milder than that of the SVD calculations. Further metadata are also provided in Figure 3.

Algorithm	Setting: $r = 5$.		Setting: $r = 20$.	
	$\frac{\ \hat{X} - X^*\ _F}{\ X^*\ _F}$	Time	$\frac{\ \hat{X} - X^*\ _F}{\ X^*\ _F}$	Time
RSVP	5.15e-05	0.78	1.86e-05	0.38
SparseApproxSDP	4.63e-03	3.74	2.25e-03	4.38
AccUniPDGrad	4.04e-05	0.36	2.41e-05	0.33
ProjFGD	2.41e-05	0.06	1.61e-05	0.04

Figure 3: Results for reconstruction and efficiency. Time reported is in seconds. For all cases, $C_{\text{sam}} = 3$ and $q = 10$.

problem is matrix-matrix and matrix-vector multiplications. convergence in terms of # of iterations, this overall results into faster convergence towards a good approximation of X^* , even as the dimension increases. Figure 4(right) shows how the total execution time scales with parameter r .

Overall performance. **ProjFGD** shows a competitive performance, as compared to the state-of-the-art algorithms; we would like to emphasize also that projected gradient descent schemes, such as [7], are also efficient in small- to medium-sized problems, due to their fast convergence rate. Moreover, convex approaches might show better sampling complexity performance (*i.e.*, as C_{sam} decreases). For more experimental results, we defer the reader to Appendix, due to space restrictions.

Setting: $q = 13$, $C_{\text{sam}} = 3$.		
Algorithm	$\frac{\ \hat{X} - X^*\ _F}{\ X^*\ _F}$	Time
AccUniPDGrad	8.5262e-05	2354.4552
ProjFGD	9.7410e-06	1214.0654

Figure 2: Comparison results for reconstruction and efficiency. Time reported is in seconds.

For completeness, in the appendix we also provide results that illustrate the effect of random initialization: Similar to above, **ProjFGD** shows competitive behavior by finding a better solution faster, irrespective of initialization point.

Timing evaluation (total and per iteration). Figure 4 highlights the efficiency of our algorithm in terms of time complexity, for various problem configurations. Our algorithm has fairly low per iteration complexity (where the most expensive operation for this

(where the most expensive operation for this

Since our algorithm shows also fast convergence in terms of # of iterations, this overall results into faster convergence towards a good approximation of X^* , even as the dimension increases. Figure 4(right) shows how the total execution time scales with parameter r .

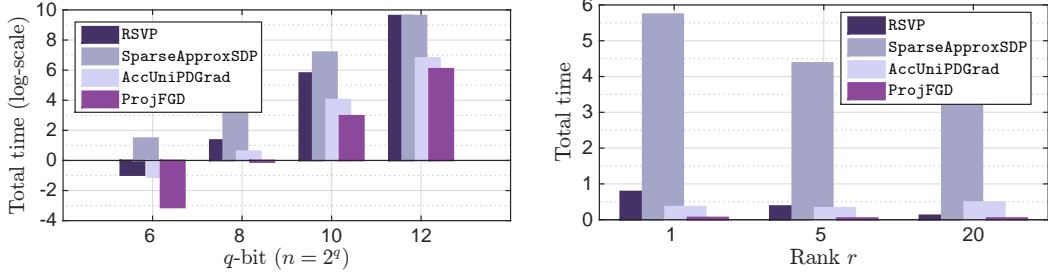


Figure 4: Timing bar plot: y -axis shows total execution time (**log-scale**) and x -axis corresponds to different q values. Left panel corresponds to $r = 1$ and $C_{\text{sam}} = 6$; right panel corresponds to $q = 10$ and $C_{\text{sam}} = 6$.

4.2 Sparse phase retrieval

Consider the sparse phase retrieval (SPR) problem [16, 14, 33]: we are interested in recovering a (sparse) unknown vector $x^* \in \mathbb{C}^n$, via its *lifted*, rank-1 representation $X^* = x^*x^{*H} \in \mathbb{C}^{n \times n}$, from a set of quadratic measurements:

$$y_i = \text{TR}(a_i^H X a_i) + \eta_i, \quad i = 1, \dots, m.$$

Here, $a_i \in \mathbb{C}^n$ are given measurement vectors (often Fourier vectors) and η_i is an additive error term. The above description leads to the following non-convex optimization criterion:

$$\begin{aligned} & \underset{X \succeq 0}{\text{minimize}} \quad \|\mathcal{A}(X) - y\|_F^2, \\ & \text{subject to} \quad \text{rank}(X) = 1, (\|X\|_1 \leq \lambda). \end{aligned} \tag{13}$$

Here, $\mathcal{A} : \mathbb{C}^{n \times n} \rightarrow \mathbb{C}^m$ such that $(\mathcal{A}(X))_i = \text{TR}(\Phi_i X)$ where $\Phi_i = a_i a_i^H$. In the case where we know x^* is sparse [33, 39], we can further constrain the lifted variable X to satisfy $\|X\|_1 \leq \lambda$, $\lambda > 0$; this way we implicitly also restrict the number of non-zeros in its factors and can recover X^* from a *limited* set of measurements.

Transforming (13) into a factored formulation. Given the rule $X = uu^H$, where $u \in \mathbb{C}^n$, one can consider the factored problem re-formulation:

$$\begin{aligned} & \underset{u \in \mathbb{C}^n}{\text{minimize}} \quad \|\mathcal{A}(uu^H) - y\|_F^2 \\ & \text{subject to} \quad \|u\|_1 \leq \lambda'. \end{aligned} \tag{14}$$

for some $\lambda' > 0$.

Remark 1. *In contrast to the QST problem, where there is a continuous map between the constraints in the original X space and in the factored U space (i.e., $\text{TR}(X) \leq \lambda \Leftrightarrow \|U\|_F^2 \leq \lambda$), this is not true for the SPR problem: As we state in the main text, points $U \in \mathcal{C}$ can result into $X \notin \mathcal{C}'$, depending on the selection of λ, λ' values (i.e., \mathcal{C} is unfaithful). In this case, the convergence theorem 3.1 in the U factor space only proves convergence to a point U^* in the factored space, which is not necessarily related to the optimal point X^* in the original space. However, as we show next, in practice, even in this case ProjFGD returns a competitive (if not better) solution, compared to state-of-the-art approaches.*

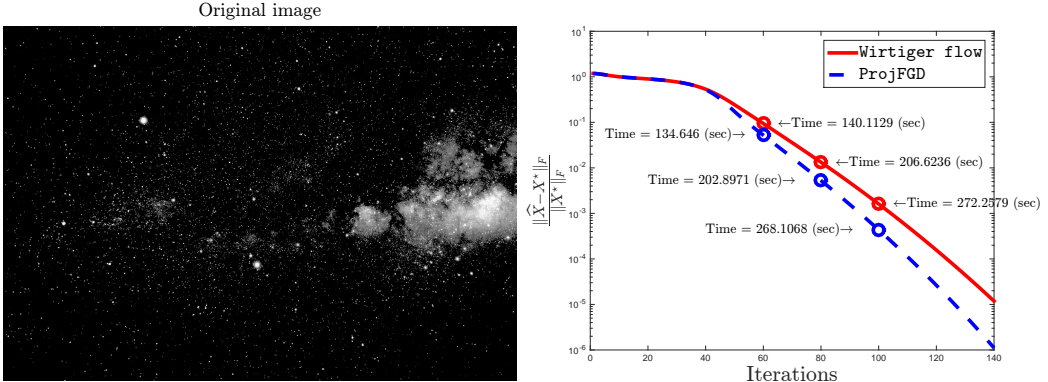


Figure 5: Left panel: Original image for the sparse phase retrieval problem. The dimension of the image is $883 \times 1280 = 1,130,240$ variables. Right panel: Convergence performance of algorithms under comparison w.r.t. $\frac{\|\hat{X} - X^*\|_F}{\|X^*\|_F}$ vs. the total number of iterations; markers on top of curves indicate the total execution time until that point.

State-of-the-art approaches. One of the most widely used methods for the phase retrieval problem comes from the seminal work of Gerchberg-Saxton [22] and Fienup [19]: they propose a greedy scheme that alternates projections on the range of $\{a_i\}_{i=1}^m$ and on the non-convex set of vectors b such that $b = |Ax|$. Main disadvantage of such greedy methods is that often they get stuck to locally minimum points.

An popularized alternative to these greedy methods is via *semidefinite relaxations*. [14] proposes **PhaseLift**, where the rank constraint is replaced by the nuclear norm surrogate. However, it is well-known that such SDP relaxations can be computationally prohibitive, when solved using off-the-self software packages, even for small problem instances; some specialized and more efficient convex relaxation algorithms are given in [21].

In [15], the authors present **Wirtinger Flow** algorithm, a non-convex scheme for solving phase retrieval problems. Similar to our approach, **Wirtinger Flow** consists of three components: (i) a careful initialization step using a spectral method, (ii) a specialized step size selection and, (iii) a recursion where gradient steps on the factored variable space are performed. Other approaches include Approximate Message Passing algorithms [41] and ADMM approaches [39].

Numerical results. We test our algorithm on image recovery, according to the description given in [15, Section 4.2]. Here, we consider grayscale images that are by nature also sparse (Figure 5 - left panel). This way, we can also consider ℓ_1 -norm constraints, as in the criterion (14). We generate $L = 21$ random octanary patterns and, using these 21 samples, we obtain the coded diffraction patterns using the grayscale image as input. As dictated by [15, Section 4.2], we perform 50 power method iterations for initialization.

For this experiment, we highlight (i) how our algorithm **ProjFGD** performs in practice, and (ii) how the additional sparsity constraint could lead to better performance. Figure 5 (right panel) depicts the relative error $\frac{\|\hat{X} - X^*\|_F}{\|X^*\|_F}$ w.r.t. the iteration count for two algorithms: (i) **Wirtinger flow** [15], and (ii) **ProjFGD**. We observe that **ProjFGD** shows a slightly better performance, compared to **Wirtinger flow**, both in terms of iterations –i.e., we reach to a better solution within the same number of iterations– and in terms of execution time –i.e., given a time wall, **ProjFGD** returns an estimate of better quality within the same amount of time. We note that both algorithms used step sizes that were slightly different in values, while **ProjFGD** further performs also a projection step.¹² Figure 6 shows some

¹²The step size in **Wirtinger flow** satisfies $\eta := \frac{\mu_t}{\|U_0\|_F^2}$, for $\mu_t = \min \left\{ 1 - e^{t/t_0}, 0.4 \right\}$ and $t_0 \approx 330$.

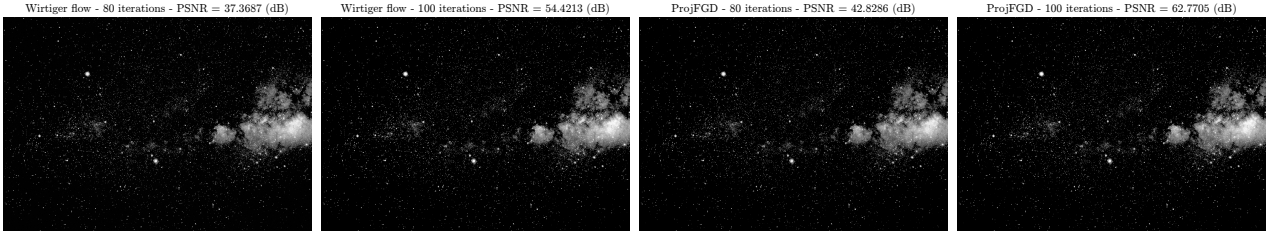


Figure 6: First two figures: Reconstructed image by using **Wirtiger flow** algorithm after 80 iterations (left panel) and 100 iterations (right panel). Last two figures: Reconstructed image by using **ProjFGD** algorithm after 80 iterations (left panel) and 100 iterations (right panel).

reconstructed images returned by the algorithms under comparison, during their execution. In all cases, both algorithms perform appealingly, finding a good approximation of the original image in less than 5 minutes; comparing the two algorithms, we note that **ProjFGD** returns a solution, within the same number of iterations, with at least 5 dB higher Peak Signal to Noise Ration (PSNR), in less time.

5 Discussion

We consider a class of low-rank matrix problems where the solution is assumed PSD and the constraint set is simple enough, according to definition in (6). This paper proposes **ProjFGD**, a non-convex projected gradient descent algorithm that operates on the factors of the PSD putative solution. When the objective function is smooth and strongly convex in the original variable space, **ProjFGD** has (local) linear rate convergence guarantees (which can become global, given a proper initialization).

The main shortcoming of our current analysis lies in the assumption that the constraint set is *simple enough*; extending the proof for more complex constraints sets is one possible research direction for future work, where an analogous of *gradient mapping* [37] might be required. Furthermore, considering barrier functions in the objective function, in order to accommodate the constraints, could be a possible extension. We hope this work will trigger future attempts along these directions.

References

- [1] S. Aaronson. The learnability of quantum states. In *Proceedings of the Royal Society of London A: Mathematical, Physical and Engineering Sciences*, volume 463, pages 3089–3114, 2007.
- [2] A. Agarwal, S. Negahban, and M. Wainwright. Fast global convergence rates of gradient methods for high-dimensional statistical recovery. In *Advances in NIPS*, pages 37–45, 2010.
- [3] S. Balakrishnan, M. Wainwright, and B. Yu. Statistical guarantees for the EM algorithm: From population to sample-based analysis. *arXiv preprint arXiv:1408.2156*, 2014.
- [4] L. Balzano, R. Nowak, and B. Recht. Online identification and tracking of subspaces from highly incomplete information. In *Communication, Control, and Computing (Allerton), 2010 48th Annual Allerton Conference on*, pages 704–711. IEEE, 2010.
- [5] S. Becker, J. Bobin, and E. Candès. NESTA: A fast and accurate first-order method for sparse recovery. *SIAM Journal on Imaging Sciences*, 4(1):1–39, 2011.
- [6] S. Becker, E. Candès, and M. Grant. Templates for convex cone problems with applications to sparse signal recovery. *Mathematical Programming Computation*, 3(3):165–218, 2011.
- [7] S. Becker, V. Cevher, and A. Kyriolidis. Randomized low-memory singular value projection. In *10th International Conference on Sampling Theory and Applications (Sampta)*, 2013.
- [8] S. Bhojanapalli, A. Kyriolidis, and S. Sanghavi. Dropping convexity for faster semi-definite optimization. *arXiv preprint arXiv:1509.03917*, 2015.

- [9] N. Boumal and P.-A. Absil. RTRMC: A Riemannian trust-region method for low-rank matrix completion. In *Advances in neural information processing systems*, pages 406–414, 2011.
- [10] S. Bubeck. Theory of convex optimization for machine learning. *arXiv preprint arXiv:1405.4980*, 2014.
- [11] S. Burer and R. Monteiro. A nonlinear programming algorithm for solving semidefinite programs via low-rank factorization. *Mathematical Programming*, 95(2):329–357, 2003.
- [12] S. Burer and R. Monteiro. Local minima and convergence in low-rank semidefinite programming. *Mathematical Programming*, 103(3):427–444, 2005.
- [13] J. Cai, E. Candès, and Z. Shen. A singular value thresholding algorithm for matrix completion. *SIAM Journal on Optimization*, 20(4):1956–1982, 2010.
- [14] E. Candes, Y. Eldar, T. Strohmer, and V. Voroninski. Phase retrieval via matrix completion. *SIAM Review*, 57(2):225–251, 2015.
- [15] E. Candes, X. Li, and M. Soltanolkotabi. Phase retrieval via Wirtinger flow: Theory and algorithms. *Information Theory, IEEE Transactions on*, 61(4):1985–2007, 2015.
- [16] E. Candes, T. Strohmer, and V. Voroninski. Phaselift: Exact and stable signal recovery from magnitude measurements via convex programming. *Communications on Pure and Applied Mathematics*, 66(8):1241–1274, 2013.
- [17] Y. Chen, S. Bhojanapalli, S. Sanghavi, and R. Ward. Coherent matrix completion. In *Proceedings of The 31st International Conference on Machine Learning*, pages 674–682, 2014.
- [18] Y. Chen and M. Wainwright. Fast low-rank estimation by projected gradient descent: General statistical and algorithmic guarantees. *arXiv preprint arXiv:1509.03025*, 2015.
- [19] C. Fienup and J. Dainty. Phase retrieval and image reconstruction for astronomy. *Image Recovery: Theory and Application*, pages 231–275, 1987.
- [20] S. Flammia, D. Gross, Y.-K. Liu, and J. Eisert. Quantum tomography via compressed sensing: Error bounds, sample complexity and efficient estimators. *New Journal of Physics*, 14(9):095022, 2012.
- [21] F. Fogel, I. Waldspurger, and A. d’Aspremont. Phase retrieval for imaging problems. *arXiv preprint arXiv:1304.7735*, 2013.
- [22] R. Gerchberg. A practical algorithm for the determination of phase from image and diffraction plane pictures. *Optik*, 35:237, 1972.
- [23] D. Gross, Y.-K. Liu, S. Flammia, S. Becker, and J. Eisert. Quantum state tomography via compressed sensing. *Physical review letters*, 105(15):150401, 2010.
- [24] M. Hardt and M. Wootters. Fast matrix completion without the condition number. In *Proceedings of The 27th Conference on Learning Theory*, pages 638–678, 2014.
- [25] E. Hazan. Sparse approximate solutions to semidefinite programs. In *LATIN 2008: Theoretical Informatics*, pages 306–316. Springer, 2008.
- [26] K. Jaganathan, S. Oymak, and B. Hassibi. Sparse phase retrieval: Convex algorithms and limitations. In *Information Theory Proceedings (ISIT)*, pages 1022–1026. IEEE, 2013.
- [27] P. Jain, R. Meka, and I. Dhillon. Guaranteed rank minimization via singular value projection. In *Advances in Neural Information Processing Systems*, pages 937–945, 2010.
- [28] P. Jain, P. Netrapalli, and S. Sanghavi. Low-rank matrix completion using alternating minimization. In *Proceedings of the 45th annual ACM symposium on Symposium on theory of computing*, pages 665–674. ACM, 2013.
- [29] A. Kalev, R. Kosut, and I. Deutsch. Quantum tomography protocols with positivity are compressed sensing protocols. *Nature partner journals (npj) Quantum Information*, 1:15018, 2015.
- [30] A. Kyrillidis and V. Cevher. Matrix recipes for hard thresholding methods. *Journal of mathematical imaging and vision*, 48(2):235–265, 2014.

- [31] S. Laue. A hybrid algorithm for convex semidefinite optimization. In *Proceedings of the 29th International Conference on Machine Learning (ICML-12)*, pages 177–184, 2012.
- [32] K. Lee and Y. Bresler. ADMiRA: Atomic decomposition for minimum rank approximation. *Information Theory, IEEE Transactions on*, 56(9):4402–4416, 2010.
- [33] X. Li and V. Voroninski. Sparse signal recovery from quadratic measurements via convex programming. *SIAM Journal on Mathematical Analysis*, 45(5):3019–3033, 2013.
- [34] Z. Lin, M. Chen, and Y. Ma. The augmented Lagrange multiplier method for exact recovery of corrupted low-rank matrices. *arXiv preprint arXiv:1009.5055*, 2010.
- [35] Y.-K. Liu. Universal low-rank matrix recovery from Pauli measurements. In *Advances in Neural Information Processing Systems*, pages 1638–1646, 2011.
- [36] L. Mirsky. A trace inequality of John von Neumann. *Monatshefte für Mathematik*, 79(4):303–306, 1975.
- [37] Y. Nesterov. *Introductory lectures on convex optimization: A basic course*, volume 87. Springer Science & Business Media, 2013.
- [38] H. Ohlsson, A. Yang, R. Dong, and S. Sastry. CPRL – an extension of compressive sensing to the phase retrieval problem. In *Advances in Neural Information Processing Systems*, pages 1376–1384, 2012.
- [39] H Ohlsson, A. Yang, R. Dong, and S. Sastry. CPRL – an extension of compressive sensing to the phase retrieval problem. In *Advances in Neural Information Processing Systems 25*, pages 1376–1384, 2012.
- [40] B. Recht, M. Fazel, and P. Parrilo. Guaranteed minimum-rank solutions of linear matrix equations via nuclear norm minimization. *SIAM review*, 52(3):471–501, 2010.
- [41] P. Schniter and S. Rangan. Compressive phase retrieval via generalized approximate message passing. *Signal Processing, IEEE Transactions on*, 63(4):1043–1055, 2015.
- [42] Y. Shechtman, A. Beck, and Y. Eldar. GESPAR: Efficient phase retrieval of sparse signals. *Signal Processing, IEEE Transactions on*, 62(4):928–938, 2014.
- [43] J. Tanner and K. Wei. Normalized iterative hard thresholding for matrix completion. *SIAM Journal on Scientific Computing*, 35(5):S104–S125, 2013.
- [44] S. Tu, R. Boczar, M. Soltanolkotabi, and B. Recht. Low-rank solutions of linear matrix equations via Procrustes flow. *arXiv preprint arXiv:1507.03566*, 2015.
- [45] Z. Wen, W. Yin, and Y. Zhang. Solving a low-rank factorization model for matrix completion by a nonlinear successive over-relaxation algorithm. *Mathematical Programming Computation*, 4(4):333–361, 2012.
- [46] A. Yurtsever, Q. Tran-Dinh, and V. Cevher. A universal primal-dual convex optimization framework. In *Advances in Neural Information Processing Systems 28*, pages 3132–3140. 2015.
- [47] D. Zhang and L. Balzano. Global convergence of a grassmannian gradient descent algorithm for subspace estimation. *arXiv preprint arXiv:1506.07405*, 2015.
- [48] T. Zhao, Z. Wang, and H. Liu. A nonconvex optimization framework for low rank matrix estimation. In *Advances in Neural Information Processing Systems 28*, pages 559–567. 2015.
- [49] Q. Zheng and J. Lafferty. A convergent gradient descent algorithm for rank minimization and SDP from random linear measurements. In *Advances in NIPS*, pages 109–117, 2015.

6 Additional experiments

6.1 Quantum state tomography – more results

Figures 7-8 show further results regarding the QST problem, where $r = 1$ and $q = 10, 12$, respectively. For each case, we present both the performance in terms of number of iterations needed, as well as what is the cumulative time required. For all algorithms, we use as initial point $U_0 = \Pi_C(\widetilde{U}_0)$ such that $X_0 = \widetilde{U}_0 \widetilde{U}_0^\top$ where $X_0 = \Pi_+(-\mathcal{A}^*(y))$ and $\Pi_+(\cdot)$ is the projection onto the PSD cone. Configurations

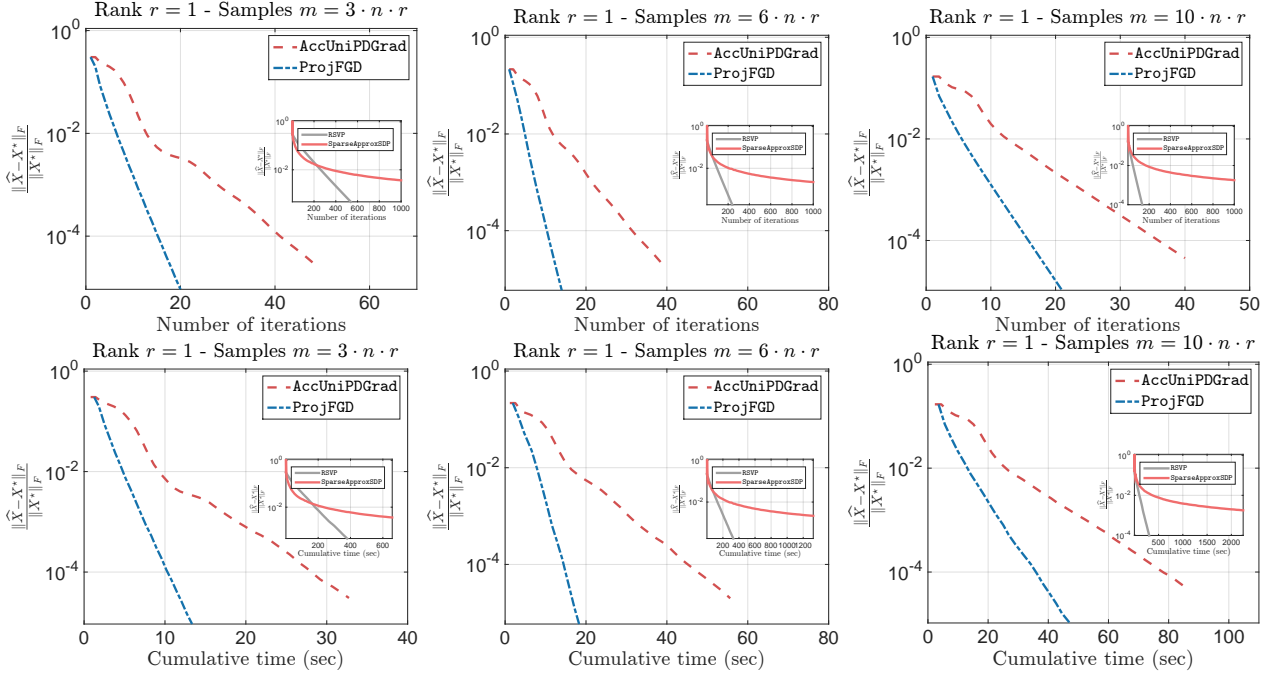


Figure 7: **Quantum state tomography:** Convergence performance of algorithms under comparison w.r.t. $\frac{\|\hat{X} - X^*\|_F}{\|X^*\|_F}$ vs. (i) the total number of iterations (top) and (ii) the total execution time (sec). First, second and third column corresponds to $C_{\text{sam}} = 3, 6$ and 10 , respectively. For all cases, $r = 1$ (pure state setting) and $q = 10$. Initial point is $U_0 = \Pi_C(\tilde{U}_0)$ such that $X_0 = \tilde{U}_0 \tilde{U}_0^\top$ where $X_0 = \Pi_+(-\mathcal{A}^*(y))$.

are described in the caption of each figure. Table 1 contains information regarding total time required for convergence and quality of solution for all these cases. Results on almost pure density states, *i.e.*, $r > 1$, are provided in Figure 9.

For completeness, we also provide results that illustrate the effect of initialization. In this case, we consider a random initialization and the same initial point is used for all algorithms. Some results are illustrated in Figure 10; table 2 contains metadata of these experiments. Similar to above, ProjFGD shows competitive behavior by finding a better solution faster, irrespective of initialization point.

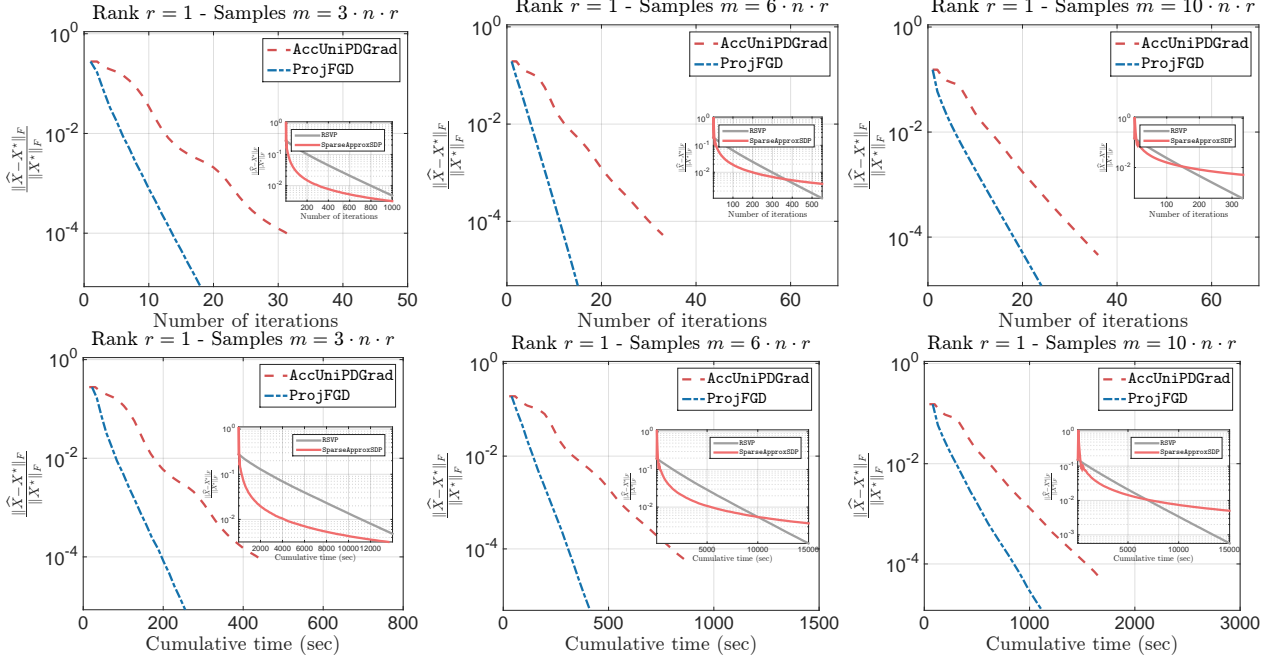


Figure 8: **Quantum state tomography:** Convergence performance of algorithms under comparison w.r.t. $\frac{\|\hat{X} - X^*\|_F}{\|X^*\|_F}$ vs. (i) the total number of iterations (top) and (ii) the total execution time (bottom). First, second and third column corresponds to $C_{\text{sam}} = 3, 6$ and 10 , respectively. For all cases, $r = 1$ (pure state setting) and $q = 12$. Initial point is $U_0 = \Pi_C(\tilde{U}_0)$ such that $X_0 = \tilde{U}_0 \tilde{U}_0^\top$ where $X_0 = \Pi_+(-\mathcal{A}^*(y))$.

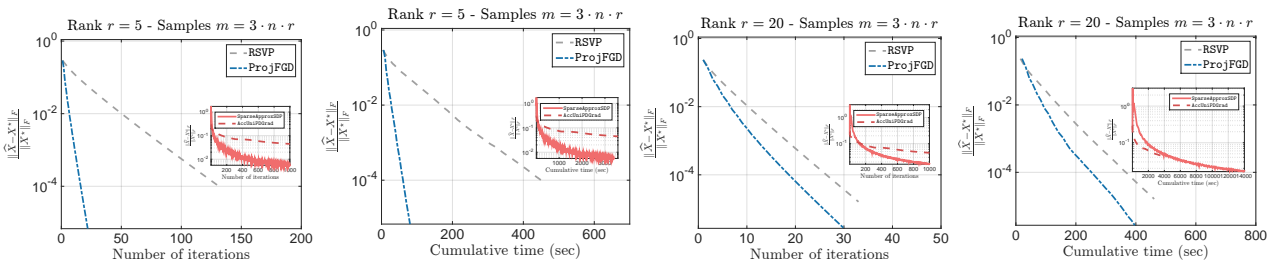


Figure 9: **Quantum state tomography:** Convergence performance of algorithms under comparison w.r.t. $\frac{\|\hat{X} - X^*\|_F}{\|X^*\|_F}$ vs. (i) the total number of iterations (left) and (ii) the total execution time (right). The two left plots correspond to the case $r = 5$ and the two right plots to the case $r = 20$. In all cases $C_{\text{sam}} = 3$ and $q = 10$. Initial point is $U_0 = \Pi_C(\tilde{U}_0)$ such that $X_0 = \tilde{U}_0 \tilde{U}_0^\top$ where $X_0 = \Pi_+(-\mathcal{A}^*(y))$.

Algorithm	$q = 6, C_{\text{sam}} = 3$		$q = 6, C_{\text{sam}} = 6$		$q = 6, C_{\text{sam}} = 10$	
	$\frac{\ \hat{X} - X^*\ _F}{\ X^*\ _F}$	Total time	$\frac{\ \hat{X} - X^*\ _F}{\ X^*\ _F}$	Total time	$\frac{\ \hat{X} - X^*\ _F}{\ X^*\ _F}$	Total time
RSVP	5.1496e-05	0.7848	1.8550e-05	0.3791	6.6328e-06	0.1203
SparseApproxSDP	4.6323e-03	3.7404	2.2469e-03	4.3775	1.4776e-03	3.8536
AccUniPDGrad	4.0388e-05	0.3634	2.4064e-05	0.3311	1.9032e-05	0.4911
ProjFGD	2.4116e-05	0.0599	1.6052e-05	0.0441	1.1419e-05	0.0446
$q = 8, C_{\text{sam}} = 3$		$q = 8, C_{\text{sam}} = 6$		$q = 8, C_{\text{sam}} = 10$		
RSVP	1.5774e-04	5.7347	5.2470e-05	3.8649	2.9583e-05	4.6548
SparseApproxSDP	4.1639e-03	16.1074	2.2011e-03	33.7608	1.7631e-03	85.0633
AccUniPDGrad	3.5122e-05	1.1006	2.4634e-05	1.8428	1.7719e-05	3.9440
ProjFGD	2.4388e-05	0.6918	1.5431e-05	0.8994	1.0561e-05	1.8804
$q = 10, C_{\text{sam}} = 3$		$q = 10, C_{\text{sam}} = 6$		$q = 10, C_{\text{sam}} = 10$		
RSVP	4.6056e-04	379.8635	1.8017e-04	331.1315	9.7585e-05	307.9554
SparseApproxSDP	3.6310e-03	658.7082	2.1911e-03	1326.5374	1.7687e-03	2245.2301
AccUniPDGrad	3.0456e-05	33.3585	1.9931e-05	56.9693	4.5022e-05	88.2965
ProjFGD	9.2352e-06	13.9547	5.8515e-06	19.3982	1.0460e-05	49.4528
$q = 12, C_{\text{sam}} = 3$		$q = 12, C_{\text{sam}} = 6$		$q = 12, C_{\text{sam}} = 10$		
RSVP	4.7811e-03	14029.1525	1.0843e-03	15028.2836	5.6169e-04	15067.7249
SparseApproxSDP	3.1717e-03	13635.4238	3.6954e-03	15041.6235	5.0197e-03	15051.4497
AccUniPDGrad	8.8050e-05	461.2084	5.2367e-05	904.0507	4.5660e-05	1759.6698
ProjFGD	8.4761e-06	266.8203	4.7399e-06	440.7193	1.1871e-05	1159.2885

Table 1: **Quantum state tomography:** Summary of comparison results for reconstruction and efficiency. As a stopping criterion, we used $\|X_{i+1} - X_i\|_2 / \|X_{i+1}\|_2 \leq 5 \cdot 10^{-6}$, where X_i is the estimate at the i -th iteration. Time reported is in seconds. Initial point is $U_0 = \Pi_{\mathcal{C}}(\widetilde{U}_0)$ such that $X_0 = \widetilde{U}_0 \widetilde{U}_0^\top$ where $X_0 = \Pi_+(-\mathcal{A}^*(y))$.

Algorithm	$q = 10, C_{\text{sam}} = 3$		$q = 10, C_{\text{sam}} = 6$		$q = 10, C_{\text{sam}} = 10$	
	$\frac{\ \hat{X} - X^*\ _F}{\ X^*\ _F}$	Total time	$\frac{\ \hat{X} - X^*\ _F}{\ X^*\ _F}$	Total time	$\frac{\ \hat{X} - X^*\ _F}{\ X^*\ _F}$	Total time
RSVP	4.5667e-04	545.5525	1.8550e-05	0.3791	1.5774e-04	5.7347
SparseApproxSDP	3.7592e-03	646.3486	2.2469e-03	4.3775	4.1639e-03	16.1074
AccUniPDGrad	3.6465e-05	24.8531	2.4064e-05	0.3311	3.5122e-05	1.1006
ProjFGD	7.0096e-06	19.5502	1.6052e-05	0.0441	2.4388e-05	0.6918

Table 2: **Quantum state tomography:** Summary of comparison results for reconstruction and efficiency for **random initialization**. As a stopping criterion, we used $\|X_{i+1} - X_i\|_2 / \|X_{i+1}\|_2 \leq 5 \cdot 10^{-6}$, where X_i is the estimate at the i -th iteration. Time reported is in seconds.

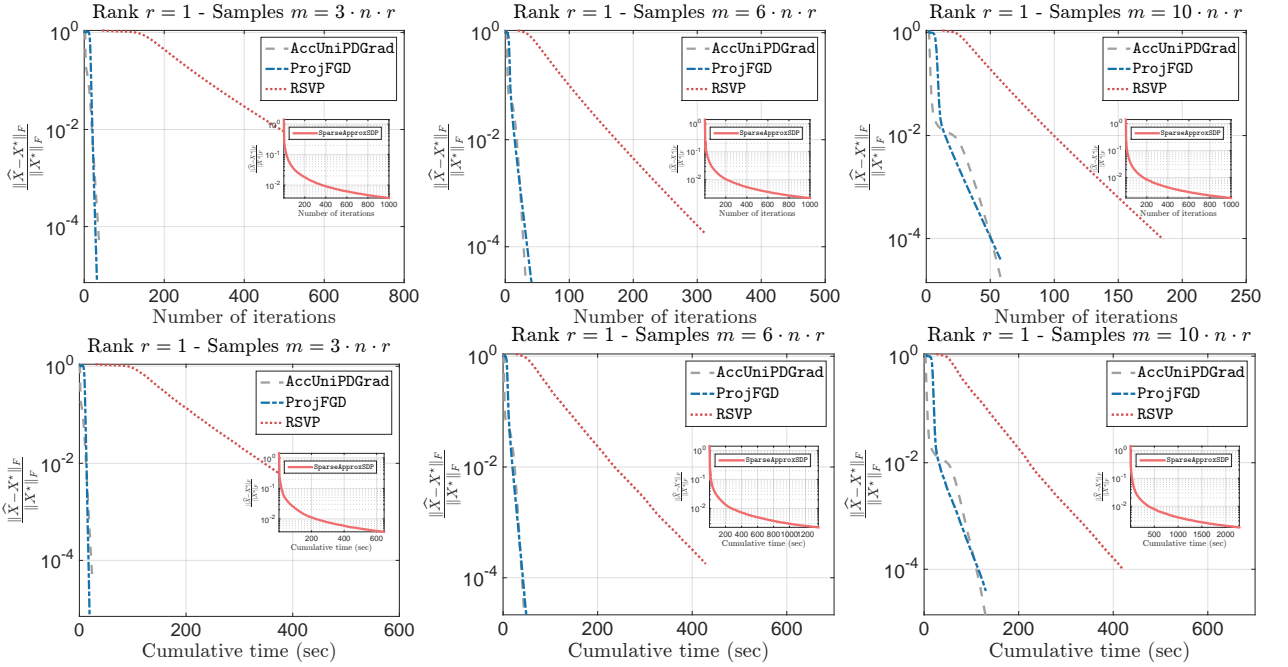


Figure 10: **Quantum state tomography:** Convergence performance of algorithms under comparison w.r.t. $\frac{\|\hat{X} - X^*\|_F}{\|X^*\|_F}$ vs. (i) the total number of iterations (left) and (ii) the total execution time (sec). All results correspond to executions starting from a **random initialization** (but common to all algorithms). In all cases $r = 1$ and $q = 10$.

7 Proofs of local convergence of the ProjFGD

Here, we present the full proof of Theorem 3.1. For clarity, we re-state the problem settings: We consider problem cases such as

$$\underset{X \in \mathbb{R}^{n \times n}}{\text{minimize}} \quad f(X) \quad \text{subject to} \quad X \succeq 0, \quad X \in \mathcal{C}'. \quad (15)$$

We assume the optimum X^* satisfies $\text{rank}(X^*) = r^*$. For our analysis, we assume we know r^* and set $r^* \equiv r$. We solve (15) in the factored space, by considering the criterion:

$$\underset{U \in \mathbb{R}^{n \times r}}{\text{minimize}} \quad f(UU^\top) \quad \text{subject to} \quad U \in \mathcal{C}. \quad (16)$$

By faithfulness of \mathcal{C} (Definition 2.4), we assume that $\mathcal{E} \subseteq \mathcal{C}$. This means that the feasible set \mathcal{C} in (16) contains all matrices U^* that lead to $X^* = U^*U^{*\top}$ in (15). Moreover, we assume both \mathcal{C} , \mathcal{C}' are convex sets and there exists a “mapping” of \mathcal{C}' onto \mathcal{C} , such that the two constraints are “equivalent”: for any $U \in \mathcal{C}$, we are guaranteed that $X = UU^\top \in \mathcal{C}'$. We restrict our discussion on norm-based sets for \mathcal{C} such that (6) is satisfied. As a representative example, in our analysis consider the case where, for any $X = UU^\top$, $\text{Tr}(X) \leq 1 \Leftrightarrow \|U\|_F^2 \leq 1$.

For our analysis, we will use the following step sizes:

$$\hat{\eta} = \frac{1}{128(L\|X_t\|_2 + \|Q_{U_t}Q_{U_t}^\top \nabla f(X_t)\|_2)}, \quad \eta^* = \frac{1}{128(L\|X^*\|_2 + \|\nabla f(X^*)\|_2)}.$$

By Lemma A.5 in [8], we know that $\hat{\eta} \geq \frac{5}{6}\eta$ and $\frac{10}{11}\eta^* \leq \eta \leq \frac{11}{10}\eta^*$. In our proof, we will work with step size $\hat{\eta}$, which is equivalent –up to constants– to the original step size η in the algorithm.

For ease of exposition, we re-define the sequence of updates: U_t is the current estimate in the factored space, $\tilde{U}_{t+1} = U_t - \hat{\eta}\nabla f(X_t)U_t$ is the putative solution after the gradient step (observe that \tilde{U}_{t+1} might belong in \mathcal{C}), and $U_{t+1} = \Pi_{\mathcal{C}}(\tilde{U}_{t+1})$ is the projection step onto \mathcal{C} . Observe that for the constraint cases we consider in this paper, $U_{t+1} = \Pi_{\mathcal{C}}(\tilde{U}_{t+1}) = \xi_t(\tilde{U}_{t+1}) \cdot \tilde{U}_{t+1}$, where $\xi_t(\cdot) \in (0, 1)$; in the case $\xi_t(\cdot) = 1$, the algorithm boils down to the FGD algorithm. For simplicity, we drop the subscript and the parenthesis of the ξ parameter; these values are apparent from the context.

We assume that ProjFGD is initialized with a “good” starting point $X_0 = U_0U_0^\top$, such that:

$$(A1) \quad U_0 \in \mathcal{C} \quad \text{and} \quad \text{DIST}(U_0, U^*) \leq \rho'\sigma_r(U^*) \quad \text{for} \quad \rho' := c \cdot \frac{\mu}{L} \cdot \frac{\sigma_r(X^*)}{\sigma_1(X^*)}, \quad \text{where } c \leq \frac{1}{200}.$$

By the assumptions above, $X_0 = U_0U_0^\top \in \mathcal{C}'$. Next, we show that the above lead to a local convergence result. A practical initialization procedure is given in Section 8 and follows from [8]; this also is used in the experimental section 4.

7.1 Proof of Theorem 3.1

For our analysis, we make use of the following lemma [10, Chapter 3], which characterizes the effect of projections onto convex sets w.r.t. to inner products, as well as provides a type-of triangle inequality for such projections; see also Figure 11 for a simple illustration.

Lemma 7.1. *Let $U \in \mathcal{C} \subseteq \mathbb{R}^{n \times r}$ and $V \in \mathbb{R}^{n \times r}$ where $V \notin \mathcal{C}$. Then,*

$$\langle \Pi_{\mathcal{C}}(V) - U, V - \Pi_{\mathcal{C}}(V) \rangle \geq 0. \quad (17)$$

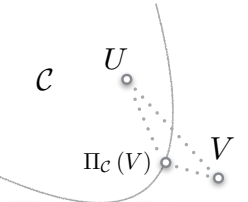


Figure 11: Illustration of Lemma 7.1

Proof of Theorem 3.1. We start with the following series of (in)equalities:

$$\begin{aligned}
\text{DIST}(U_{t+1}, U^*)^2 &= \min_{R \in \mathcal{O}} \|U_{t+1} - U^*R\|_F^2 \\
&\stackrel{(i)}{\leq} \|U_{t+1} - U^*R_{U_t}^*\|_F^2 \\
&\stackrel{(ii)}{=} \|U_{t+1} - \tilde{U}_{t+1} + \tilde{U}_{t+1} - U^*R_{U_t}^*\|_F^2 \\
&= \|U_{t+1} - \tilde{U}_{t+1}\|_F^2 + \|\tilde{U}_{t+1} - U^*R_{U_t}^*\|_F^2 \\
&\quad + 2 \langle U_{t+1} - \tilde{U}_{t+1}, \tilde{U}_{t+1} - U^*R_{U_t}^* \rangle,
\end{aligned}$$

where (i) is due to the fact $R_{U_t}^* := \text{argmin}_{R \in \mathcal{O}} \|U_t - U^*R\|_F^2$, (ii) is obtained by adding and subtracting \tilde{U}_{t+1} .

Focusing on the second term of the right hand side, we substitute \tilde{U}_{t+1} to obtain:

$$\begin{aligned}
\|\tilde{U}_{t+1} - U^*R_{U_t}^*\|_F^2 &= \|U_t - \hat{\eta} \nabla f(U_t U_t^\top) U_t - U^*R_{U_t}^*\|_F^2 \\
&= \|U_t - U^*R_{U_t}^*\|_F^2 + \hat{\eta}^2 \|\nabla f(U_t U_t^\top) U_t\|_F^2 \\
&\quad - 2\hat{\eta} \langle \nabla f(U_t U_t^\top) U_t, U_t - U^*R_{U_t}^* \rangle
\end{aligned}$$

Then, our initial equation transforms into:

$$\begin{aligned}
\text{DIST}(U_{t+1}, U^*)^2 &\leq \|U_{t+1} - \tilde{U}_{t+1}\|_F^2 + \text{DIST}(U_t, U^*)^2 + \hat{\eta}^2 \|\nabla f(U_t U_t^\top) U_t\|_F^2 \\
&\quad - 2\hat{\eta} \langle \nabla f(U_t U_t^\top) U_t, U_t - U^*R_{U_t}^* \rangle \\
&\quad + 2 \langle U_{t+1} - \tilde{U}_{t+1}, \tilde{U}_{t+1} - U^*R_{U_t}^* \rangle
\end{aligned}$$

Focusing further on the last term of the expression above, we obtain:

$$\begin{aligned}
\langle U_{t+1} - \tilde{U}_{t+1}, \tilde{U}_{t+1} - U^*R_{U_t}^* \rangle &= \langle U_{t+1} - \tilde{U}_{t+1}, \tilde{U}_{t+1} - U_{t+1} + U_{t+1} - U^*R_{U_t}^* \rangle \\
&= \langle U_{t+1} - \tilde{U}_{t+1}, \tilde{U}_{t+1} - U_{t+1} \rangle \\
&\quad + \langle U_{t+1} - \tilde{U}_{t+1}, U_{t+1} - U^*R_{U_t}^* \rangle
\end{aligned}$$

Observe that, in the special case where $\tilde{U}_{t+1} \equiv U_{t+1}$ for all t , *i.e.*, the iterates are always within \mathcal{C} before the projection step, the above equation equals to zero and the recursion is identical to that of [8][Proof of Theorem 4.2]. Here, we are more interested in the case where $\tilde{U}_{t+1} \not\equiv U_{t+1}$ for some t —thus $U_{t+1} \notin \mathcal{C}$. By faithfulness (Definition 2.1), observe that $U^*R_{U_t}^* \in \mathcal{C}$ and $X^* = U^*R_{U_t}^* (U^*R_{U_t}^*)^\top = U^*U^{*\top}$. Moreover, $U_{t+1} = \Pi_{\mathcal{C}}(\tilde{U}_{t+1})$: Then, according to Lemma 7.1 and focusing on eq. (17), for $U := U^*R_{U_t}^*$ and $V := \tilde{U}_{t+1}$, the last term in the above equation satisfies:

$$\langle U_{t+1} - \tilde{U}_{t+1}, U_{t+1} - U^*R_{U_t}^* \rangle \leq 0,$$

and, thus, the expression above becomes:

$$\langle U_{t+1} - \tilde{U}_{t+1}, \tilde{U}_{t+1} - U^*R_{U_t}^* \rangle \leq -\|U_{t+1} - \tilde{U}_{t+1}\|_F^2.$$

Therefore, going back to the original recursive expression, we obtain:

$$\begin{aligned} \text{DIST}(U_{t+1}, U^*)^2 &\leq -\|U_{t+1} - \tilde{U}_{t+1}\|_F^2 + \text{DIST}(U_t, U^*)^2 + \hat{\eta}^2 \|\nabla f(U_t U_t^\top) U_t\|_F^2 \\ &\quad - 2\hat{\eta} \left\langle \nabla f(U_t U_t^\top) U_t, U_t - U^* R_{U_t}^* \right\rangle \end{aligned}$$

For the last term, we use the descent lemma 3.3 in the main text; the proof is provided in Section 7.2. Thus, we can conclude that:

$$\text{DIST}(U_{t+1}, U^*)^2 \leq \left(1 - \frac{3\hat{\eta}\mu}{10} \cdot \sigma_r(X^*)\right) \cdot \text{DIST}(U_t, U^*)^2.$$

The expression for α is obtained by observing $\hat{\eta} \geq \frac{5}{6}\eta$ and $\frac{10}{11}\eta^* \leq \eta \leq \frac{11}{10}\eta^*$, from Lemma 20 in [8]. Then, for $\eta^* \leq \frac{C}{L\|X^*\|_2 + \|\nabla f(X^*)\|_2}$ and $C = 1/128$, we have:

$$\begin{aligned} 1 - \frac{3\hat{\eta}\mu}{10} \cdot \sigma_r(X^*) &\leq 1 - \frac{3 \cdot \frac{10}{11} \cdot \frac{5}{6}\eta^*\mu}{10} \cdot \sigma_r(X^*) \\ &= 1 - \frac{15}{66}\eta^*\mu \cdot \sigma_r(X^*) \\ &= 1 - \frac{15}{66} \frac{\mu \cdot \sigma_r(X^*)}{128(L\|X^*\|_2 + \|\nabla f(X^*)\|_2)} \\ &\leq 1 - \frac{\mu \cdot \sigma_r(X^*)}{550(L\|X^*\|_2 + \|\nabla f(X^*)\|_2)} =: \alpha \end{aligned}$$

where $\alpha < 1$.

Concluding the proof, the condition $\text{DIST}(U_{t+1}, U^*)^2 \leq \rho' \sigma_r(U^*)$ is naturally satisfied, since $\alpha < 1$. \square

7.2 Proof of Lemma 3.3

First we recall the definition of *restricted strong convexity*:

Definition 7.2. Let $f : \mathbb{R}^{n \times n} \rightarrow \mathbb{R}$ be convex and differentiable. Then, f is (μ, r) -restricted strongly convex if:

$$f(Y) \geq f(X) + \langle \nabla f(X), Y - X \rangle + \frac{\mu}{2} \|Y - X\|_F^2, \quad \forall X, Y \in \mathbb{R}^{n \times n}, \text{ rank-}r \text{ matrices.} \quad (18)$$

The statements below apply also for standard μ -strong convex functions, as defined in Definition 2.2.

Recall $\tilde{U}_{t+1} = U_t - \hat{\eta} \nabla f(X_t) U_t$ and define $\Delta := U_t - U^* R_{U_t}^*$. Before presenting the proof, we need the following lemma that bounds one of the error terms arising in the proof of Lemma 3.3. This is a variation of Lemma 6.3 in [8]. The proof is presented in Section 7.3.

Lemma 7.3. Let f be L -smooth and (μ, r) -restricted strongly convex. Then, under the assumptions of Theorem 3.1 and assuming step size $\hat{\eta} = \frac{1}{128(L\|X\|_2 + \|\nabla f(X_t) Q_{U_t} Q_{U_t}^\top\|_2)}$, the following bound holds true:

$$\left\langle \nabla f(X_t), \Delta \Delta^\top \right\rangle \geq -\frac{\hat{\eta}}{5} \|\nabla f(X_t) U_t\|_F^2 - \frac{\mu \sigma_r(X^*)}{10} \cdot \text{DIST}(U_t, U^*)^2. \quad (19)$$

Now we are ready to present the proof of Lemma 3.3.

Proof of Lemma 3.3. First we rewrite the inner product as shown below.

$$\begin{aligned}
\langle \nabla f(X_t)U_t, U_t - U^\star R_{U_t}^\star \rangle &= \left\langle \nabla f(X_t), X_t - U^\star R_{U_t}^\star U_t^\top \right\rangle \\
&= \frac{1}{2} \langle \nabla f(X_t), X_t - X^\star \rangle + \left\langle \nabla f(X_t), \frac{1}{2}(X_t + X^\star) - U^\star R_{U_t}^\star U_t^\top \right\rangle \\
&= \frac{1}{2} \langle \nabla f(X_t), X_t - X^\star \rangle + \frac{1}{2} \langle \nabla f(X_t), \Delta \Delta^\top \rangle,
\end{aligned} \tag{20}$$

which follows by adding and subtracting $\frac{1}{2}X^\star$.

Let us focus on bounding the first term on the right hand side of (20). Consider points $X_t = U_t U_t^\top$ and $X_{t+1} = U_{t+1} U_{t+1}^\top$; by assumption, both X_t and X_{t+1} are feasible points in (16). By smoothness of f , we get:

$$\begin{aligned}
f(X_t) &\geq f(X_{t+1}) - \langle \nabla f(X_t), X_{t+1} - X_t \rangle - \frac{L}{2} \|X_{t+1} - X_t\|_F^2 \\
&\stackrel{(i)}{\geq} f(X^\star) - \langle \nabla f(X_t), X_{t+1} - X_t \rangle - \frac{L}{2} \|X_{t+1} - X_t\|_F^2,
\end{aligned} \tag{21}$$

where (i) follows from optimality of X^\star and since X_{t+1} is a feasible point ($X_{t+1} \succeq 0$, $\Pi_{\mathcal{C}'}(X_{t+1}) = X_{t+1}$) for problem (15).

Moreover, by the (μ, r) -restricted strong convexity of f , we get,

$$f(X^\star) \geq f(X_t) + \langle \nabla f(X_t), X^\star - X_t \rangle + \frac{\mu}{2} \|X^\star - X_t\|_F^2. \tag{22}$$

Combining equations (21), and (22), we obtain:

$$\langle \nabla f(X_t), X_t - X^\star \rangle \geq \langle \nabla f(X_t), X_t - X_{t+1} \rangle - \frac{L}{2} \|X_{t+1} - X_t\|_F^2 + \frac{\mu}{2} \|X^\star - X_t\|_F^2 \tag{23}$$

By the nature of the projection $\Pi_{\mathcal{C}}(\cdot)$ step, it is easy to verify that

$$X_{t+1} = \xi^2 \cdot \left(X_t - \widehat{\eta} \nabla f(X_t) X_t \Lambda_t - \widehat{\eta} \Lambda_t^\top X_t^\top \nabla f(X_t)^\top \right),$$

where $\Lambda_t = I - \frac{\widehat{\eta}}{2} Q_{U_t} Q_{U_t}^\top \nabla f(X_t) \in \mathbb{R}^{n \times n}$ and $Q_{U_t} Q_{U_t}^\top$ denoting the projection onto the column space of U_t . Notice that, for step size $\widehat{\eta}$, we have

$$\Lambda_t \succ 0, \quad \sigma_1(\Lambda_t) \leq 1 + 1/256 \quad \text{and} \quad \sigma_n(\Lambda_t) \geq 1 - 1/256.$$

Using the above X_{t+1} characterization in (23), we obtain:

$$\begin{aligned}
\langle \nabla f(X_t), X_t - X^\star \rangle - \frac{\mu}{2} \|X^\star - X_t\|_F^2 + \frac{L}{2} \|X_t - X_{t+1}\|_F^2 &\stackrel{(i)}{\geq} \langle \nabla f(X_t), (1 - \xi^2) X_t \rangle + 2\widehat{\eta} \cdot \xi^2 \cdot \langle \nabla f(X_t), \nabla f(X_t) X_t \Lambda_t \rangle \\
&\stackrel{(ii)}{\geq} (1 - \xi^2) \cdot \langle \nabla f(X_t) U_t, U_t \rangle + 2\widehat{\eta} \cdot \xi^2 \cdot \text{TR}(\nabla f(X_t) \nabla f(X_t) X_t) \cdot \sigma_n(\Lambda_t) \\
&\geq (1 - \xi^2) \cdot \langle \nabla f(X_t) U_t, U_t \rangle + \frac{255 \cdot \widehat{\eta} \cdot \xi^2}{128} \|\nabla f(X_t) U_t\|_F^2,
\end{aligned} \tag{24}$$

where: (i) follows from symmetry of $\nabla f(X_t)$ and X_t and, (ii) follows from the sequence equalities and inequalities:

$$\begin{aligned}
\text{TR}(\nabla f(X_t) \nabla f(X_t) X_t \Lambda_t) &= \text{TR}(\nabla f(X_t) \nabla f(X_t) U_t U_t^\top) - \frac{\widehat{\eta}}{2} \text{TR}(\nabla f(X_t) \nabla f(X_t) U_t U_t^\top \nabla f(X_t)) \\
&\geq \left(1 - \frac{\widehat{\eta}}{2} \|Q_{U_t} Q_{U_t}^\top \nabla f(X_t)\|_2 \right) \|\nabla f(X_t) U_t\|_F^2 \\
&\geq (1 - 1/256) \|\nabla f(X_t) U_t\|_F^2.
\end{aligned}$$

Combining the above in the expression we want to lower bound: $2\widehat{\eta}\langle \nabla f(X_t) \cdot U_t, U_t - U^* R_{U_t}^* \rangle + \|U_{t+1} - \widetilde{U}_{t+1}\|_F^2$, we obtain:

$$\begin{aligned}
2\widehat{\eta}\langle \nabla f(X_t) \cdot U_t, U_t - U^* R_{U_t}^* \rangle + \|U_{t+1} - \widetilde{U}_{t+1}\|_F^2 \\
= \widehat{\eta}\langle \nabla f(X_t), X_t - X^* \rangle + \widehat{\eta}\langle \nabla f(X_t), \Delta \Delta^\top \rangle + \|U_{t+1} - \widetilde{U}_{t+1}\|_F^2 \\
\geq (1 - \xi^2) \cdot \widehat{\eta}\langle \nabla f(X_t)U_t, U_t \rangle + \frac{255\cdot\widehat{\eta}^2\cdot\xi^2}{128}\|\nabla f(X_t)U_t\|_F^2 \\
+ \frac{\widehat{\eta}\mu}{2}\|X^* - X_t\|_F^2 - \frac{\widehat{\eta}L}{2}\|X_t - X_{t+1}\|_F^2 \\
- \frac{\widehat{\eta}^2}{5}\|\nabla f(X_t)U_t\|_F^2 - \frac{\widehat{\eta}\mu\sigma_r(X^*)}{10} \cdot \text{DIST}(U_t, U^*)^2 \\
+ \|U_{t+1} - \widetilde{U}_{t+1}\|_F^2
\end{aligned} \tag{25}$$

For the last term in the above expression and given $U_{t+1} = \Pi_C(\widetilde{U}_{t+1}) = \xi \cdot \widetilde{U}_{t+1}$ for some $\xi \in (0, 1)$, we further observe:

$$\begin{aligned}
\|U_{t+1} - \widetilde{U}_{t+1}\|_F^2 &= \|\xi \cdot \widetilde{U}_{t+1} - \widetilde{U}_{t+1}\|_F^2 \\
&= (1 - \xi)^2 \cdot \|U_t\|_F^2 + (1 - \xi)^2 \widehat{\eta}^2 \cdot \|\nabla f(X_t)U_t\|_F^2 \\
&\quad - 2(1 - \xi)^2 \cdot \widehat{\eta} \cdot \langle \nabla f(X_t)U_t, U_t \rangle
\end{aligned}$$

Combining the above equality with the first term on the right hand side in (25), we obtain:

$$\begin{aligned}
&(1 - \xi^2) \cdot \widehat{\eta}\langle \nabla f(X_t)U_t, U_t \rangle + (1 - \xi)^2 \cdot \|U_t\|_F^2 + (1 - \xi)^2 \widehat{\eta}^2 \cdot \|\nabla f(X_t)U_t\|_F^2 \\
&\quad - 2(1 - \xi)^2 \cdot \widehat{\eta} \cdot \langle \nabla f(X_t)U_t, U_t \rangle = \\
&\left[(1 - \xi^2) - 2(1 - \xi)^2 \right] \cdot \widehat{\eta}\langle \nabla f(X_t)U_t, U_t \rangle + (1 - \xi)^2 \cdot \|U_t\|_F^2 + (1 - \xi)^2 \widehat{\eta}^2 \cdot \|\nabla f(X_t)U_t\|_F^2 = \\
&(3\xi - 1)(1 - \xi) \cdot \widehat{\eta}\langle \nabla f(X_t)U_t, U_t \rangle + (1 - \xi)^2 \cdot \|U_t\|_F^2 + (1 - \xi)^2 \widehat{\eta}^2 \cdot \|\nabla f(X_t)U_t\|_F^2 = \\
&\left\| \frac{3\xi - 1}{2} \cdot U_t + (1 - \xi) \cdot \widehat{\eta} \nabla f(X_t) \cdot U_t \right\|_F^2 + \left((1 - \xi)^2 - \frac{(3\xi - 1)^2}{4} \right) \|U_t\|_F^2.
\end{aligned}$$

Focusing on the first term, let $\Theta_t := I + \frac{2(1 - \xi)}{3\xi - 1} \cdot \widehat{\eta} \cdot \nabla f(X_t)Q_{U_t}Q_{U_t}^\top$; then, $\sigma_n(\Theta_t) \geq 1 - \frac{2(1 - \xi)}{3\xi - 1} \cdot \frac{1}{128}$, by the definition of $\widehat{\eta}$ and the fact that $\widehat{\eta} \leq \frac{1}{128\|\nabla f(X_t)Q_{U_t}Q_{U_t}^\top\|_2}$. Then:

$$\begin{aligned}
\left\| \frac{3\xi - 1}{2} \cdot U_t + (1 - \xi) \cdot \widehat{\eta} \nabla f(X_t) \cdot U_t \right\|_F^2 &= \left\| \frac{3\xi - 1}{2} \Theta_t \cdot U_t \right\|_F^2 \\
&\geq \frac{(3\xi - 1)^2}{4} \cdot \|U_t\|_F^2 \cdot \sigma_n(\Theta_t)^2 \\
&\geq \frac{(3\xi - 1)^2}{4} \cdot \left(1 - \frac{2(1 - \xi)}{3\xi - 1} \cdot \frac{1}{128} \right)^2 \cdot \|U_t\|_F^2
\end{aligned}$$

Combining the above, we obtain the following bound:

$$\begin{aligned}
&(1 - \xi^2) \cdot \widehat{\eta}\langle \nabla f(X_t)U_t, U_t \rangle + \|U_{t+1} - \widetilde{U}_{t+1}\|_F^2 \\
&\geq \left((1 - \xi)^2 - \frac{(3\xi - 1)^2}{4} \cdot \left(1 - \left(1 - \frac{2(1 - \xi)}{3\xi - 1} \cdot \frac{1}{128} \right)^2 \right) \right) \cdot \|U_t\|_F^2
\end{aligned}$$

The above transform (25) as follows:

$$\begin{aligned}
&2\widehat{\eta}\langle \nabla f(X_t) \cdot U_t, U_t - U^* R_{U_t}^* \rangle + \|U_{t+1} - \widetilde{U}_{t+1}\|_F^2 \\
&\geq \left(\frac{255\cdot\xi^2}{128} - \frac{1}{5} \right) \cdot \widehat{\eta}^2 \|\nabla f(X_t)U_t\|_F^2 + \frac{\widehat{\eta}\mu}{2}\|X^* - X_t\|_F^2 - \frac{\widehat{\eta}\mu\sigma_r(X^*)}{10} \cdot \text{DIST}(U_t, U^*)^2 \\
&\quad + \left((1 - \xi)^2 - \frac{(3\xi - 1)^2}{4} \cdot \left(1 - \left(1 - \frac{2(1 - \xi)}{3\xi - 1} \cdot \frac{1}{128} \right)^2 \right) \right) \cdot \|U_t\|_F^2 - \frac{\widehat{\eta}L}{2}\|X_t - X_{t+1}\|_F^2
\end{aligned} \tag{26}$$

Let us focus on the term $\frac{\hat{\eta}L}{2} \|X_t - X_{t+1}\|_F^2$; this can be bounded as follows:

$$\begin{aligned} \frac{\hat{\eta}L}{2} \|X_t - X_{t+1}\|_F^2 &= \frac{\hat{\eta}L}{2} \|U_t U_t^\top - U_{t+1} U_{t+1}^\top\|_F^2 = \frac{\hat{\eta}L}{2} \|U_t U_t^\top - U_t U_{t+1}^\top + U_t U_{t+1}^\top - U_{t+1} U_{t+1}^\top\|_F^2 \\ &= \frac{\hat{\eta}L}{2} \|U_t (U_t - U_{t+1})^\top + (U_t - U_{t+1}) U_{t+1}^\top\|_F^2 \\ &\stackrel{(i)}{\leq} \hat{\eta}L \cdot \left(\|U_t (U_t - U_{t+1})^\top\|_F^2 + \|(U_t - U_{t+1}) U_{t+1}^\top\|_F^2 \right) \\ &\stackrel{(ii)}{\leq} \hat{\eta}L (\|U_{t+1}\|_2^2 + \|U_t\|_2^2) \cdot \|U_{t+1} - U_t\|_F^2. \end{aligned}$$

where (i) is due to the identity $\|A + B\|_F^2 \leq 2\|A\|_F^2 + 2\|B\|_F^2$ and (ii) is due to the Cauchy-Schwarz inequality. By definition of U_{t+1} , we observe that:

$$\|U_{t+1}\|_2^2 = \|\xi \cdot (U_t - \hat{\eta} \nabla f(X_t) U_t)\|_2^2 \stackrel{(i)}{\leq} \xi^2 \cdot \|U_t\|_2^2 \cdot \|I - \hat{\eta} \nabla f(X_t) Q_{U_t} Q_{U_t}^\top\|_2^2 \stackrel{(ii)}{\leq} (1 + \frac{1}{128})^2 \cdot \|U_t\|_2^2.$$

where (i) is due to Cauchy-Schwarz and (ii) is obtained by substituting $\hat{\eta} \leq \frac{1}{128 \|\nabla f(X_t) Q_{U_t} Q_{U_t}^\top\|_2}$ and since $\xi \in (0, 1)$. Thus, $\frac{\hat{\eta}L}{2} \|X_t - X_{t+1}\|_F^2$ can be further bounded as follows:

$$\begin{aligned} \frac{\hat{\eta}L}{2} \|X_t - X_{t+1}\|_F^2 &\leq \hat{\eta}L \cdot \left((1 + \frac{1}{128})^2 + 1 \right) \cdot \|U_t\|_2^2 \cdot \|U_{t+1} - U_t\|_F^2 \\ &= \hat{\eta}L \cdot \left((1 + \frac{1}{128})^2 + 1 \right) \cdot \|X_t\|_2 \cdot \|U_{t+1} - U_t\|_F^2 \\ &\leq \frac{\left(1 + \frac{1}{128}\right)^2 + 1}{128} \cdot \|U_{t+1} - U_t\|_F^2 \\ &= \frac{\left(1 + \frac{1}{128}\right)^2 + 1}{128} \cdot \|\xi \cdot \tilde{U}_{t+1} - U_t\|_F^2 \\ &= \frac{\left(1 + \frac{1}{128}\right)^2 + 1}{128} \cdot \|(\xi - 1)U_t - \xi \cdot \hat{\eta} \nabla f(X_t) \cdot U_t\|_F^2 \\ &\leq (1 - \xi)^2 \cdot \frac{\left(1 + \frac{1}{128}\right)^2 + 1}{64} \cdot \|U_t\|_F^2 + \frac{\left(1 + \frac{1}{128}\right)^2 + 1}{64} \cdot \xi^2 \cdot \hat{\eta}^2 \cdot \|\nabla f(X_t) \cdot U_t\|_F^2 \end{aligned}$$

where in the last inequality we substitute $\hat{\eta}$; observe that $\hat{\eta} \leq \frac{1}{128L\|X_t\|_2}$. Combining this result with (26), we obtain:

$$\begin{aligned} &2\hat{\eta} \langle \nabla f(X_t) \cdot U_t, U_t - U^* R_{U_t}^* \rangle + \|U_{t+1} - \tilde{U}_{t+1}\|_F^2 \\ &\geq \left(\frac{255 \cdot \xi^2}{128} - \frac{1}{5} - \frac{\left(1 + \frac{1}{128}\right)^2 + 1}{64} \cdot \xi^2 \right) \cdot \hat{\eta}^2 \|\nabla f(X_t) U_t\|_F^2 + \frac{\hat{\eta}\mu}{2} \|X^* - X_t\|_F^2 - \frac{\hat{\eta}\mu\sigma_r(X^*)}{10} \cdot \text{DIST}(U_t, U^*)^2 \\ &\quad + \left((1 - \xi)^2 \cdot \left(1 - \frac{\left(1 + \frac{1}{128}\right)^2 + 1}{64} \right) - \frac{(3\xi - 1)^2}{4} \cdot \left(1 - \left(1 - \frac{2(1 - \xi)}{3\xi - 1} \cdot \frac{1}{128} \right)^2 \right) \right) \cdot \|U_t\|_F^2 \\ &\stackrel{(i)}{\geq} \hat{\eta}^2 \|\nabla f(X_t) U_t\|_F^2 + \frac{\hat{\eta}\mu}{2} \|X^* - X_t\|_F^2 - \frac{\hat{\eta}\mu\sigma_r(X^*)}{10} \cdot \text{DIST}(U_t, U^*)^2 \\ &\quad + \left((1 - \xi)^2 \cdot \left(1 - \frac{\left(1 + \frac{1}{128}\right)^2 + 1}{64} \right) - \frac{(3\xi - 1)^2}{4} \cdot \left(1 - \left(1 - \frac{2(1 - \xi)}{3\xi - 1} \cdot \frac{1}{128} \right)^2 \right) \right) \cdot \|U_t\|_F^2 \\ &\stackrel{(ii)}{\geq} \hat{\eta}^2 \|\nabla f(X_t) U_t\|_F^2 + \frac{\hat{\eta}\mu}{2} \|X^* - X_t\|_F^2 - \frac{\hat{\eta}\mu\sigma_r(X^*)}{10} \cdot \text{DIST}(U_t, U^*)^2 \end{aligned} \tag{27}$$

where (i) is due to the assumption $\xi \gtrsim 0.78$ and thus $\left(\frac{255 \cdot \xi^2}{128} - \frac{1}{5} - \frac{\left(1 + \frac{1}{128}\right)^2 + 1}{64} \cdot \xi^2 \right) \geq 1$; see also Figure 12 (left panel), and (ii) is due to the non-negativity of the constant in front of $\|U_t\|_F^2$; see also Figure 12 (right panel).

Finally, we bound $\frac{\hat{\eta}\mu}{2} \|X^* - X_t\|_F^2$ using the following Lemma by [44]:

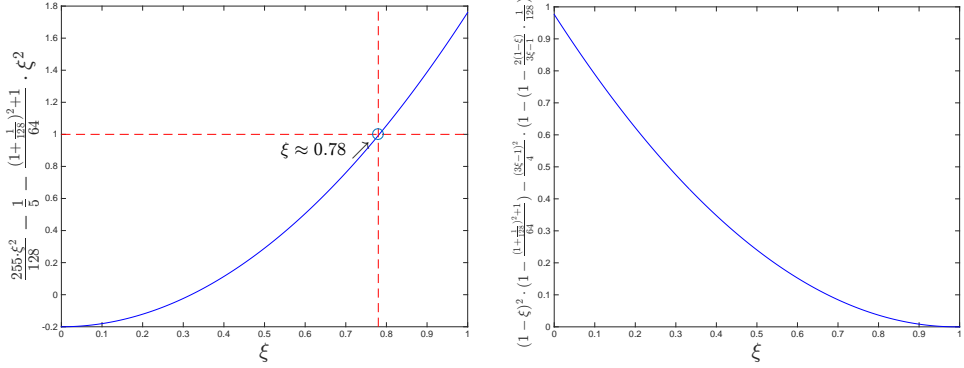


Figure 12: Behavior of constants, depending on ξ , in expression (27).

Lemma 7.4. For any $U, V \in \mathbb{R}^{n \times r}$, we have:

$$\|UU^\top - VV^\top\|^2 \geq 2 \cdot (\sqrt{2} - 1) \cdot \sigma_r(U)^2 \cdot \text{DIST}(U, V)^2.$$

Thus,

$$\frac{\hat{\eta}\mu}{2} \|X^* - X_t\|_F^2 \geq \hat{\eta}\mu \cdot (\sqrt{2} - 1) \cdot \sigma_r(X^*) \cdot \text{DIST}(U_t, U^*)^2,$$

and can thus conclude:

$$\begin{aligned} & 2\hat{\eta}\langle \nabla f(X_t) \cdot U_t, U_t - U^* R_{U_t}^* \rangle + \|U_{t+1} - \tilde{U}_{t+1}\|_F^2 \\ & \geq \hat{\eta}^2 \|\nabla f(X_t) U_t\|_F^2 + \hat{\eta}\mu \cdot (\sqrt{2} - 1) \cdot \sigma_r(X^*) \cdot \text{DIST}(U_t, U^*)^2 - \frac{\hat{\eta}\mu\sigma_r(X^*)}{10} \cdot \text{DIST}(U_t, U^*)^2 \\ & = \hat{\eta}^2 \|\nabla f(X_t) U_t\|_F^2 + \left(\sqrt{2} - 1 - \frac{1}{10}\right) \cdot \hat{\eta}\mu \cdot \sigma_r(X^*) \cdot \text{DIST}(U_t, U^*)^2 \\ & = \hat{\eta}^2 \|\nabla f(X_t) U_t\|_F^2 + \frac{3\hat{\eta}\mu}{10} \cdot \sigma_r(X^*) \cdot \text{DIST}(U_t, U^*)^2 \end{aligned}$$

This completes the proof. \square

7.3 Proof of Lemma 7.3

Proof. We can lower bound $\langle \nabla f(X_t), \Delta \Delta^\top \rangle$ as follows:

$$\begin{aligned} \langle \nabla f(X_t), \Delta \Delta^\top \rangle & \stackrel{(i)}{=} \langle Q_\Delta Q_\Delta^\top \nabla f(X_t), \Delta \Delta^\top \rangle \\ & \geq - |\text{TR} (Q_\Delta Q_\Delta^\top \nabla f(X_t) \Delta \Delta^\top)| \\ & \stackrel{(ii)}{\geq} - \|Q_\Delta Q_\Delta^\top \nabla f(X_t)\|_2 \text{TR}(\Delta \Delta^\top) \\ & \stackrel{(iii)}{\geq} - \left(\|Q_{U_t} Q_{U_t}^\top \nabla f(X_t)\|_2 + \|Q_{U^*} Q_{U^*}^\top \nabla f(X_t)\|_2 \right) \text{DIST}(U_t, U^*)^2. \end{aligned} \quad (28)$$

Note that (i) follows from the fact $\Delta = Q_\Delta Q_\Delta^\top \Delta$ and (ii) follows from $|\text{TR}(AB)| \leq \|A\|_2 \text{TR}(B)$, for PSD matrix B (Von Neumann's trace inequality [36]). For the transformation in (iii), we use that fact that the column space of Δ , $\text{SPAN}(\Delta)$, is a subset of $\text{SPAN}(U_t \cup U^*)$, as Δ is a linear combination of U_t and $U^* R_{U_t}^*$.

For the second term in the parenthesis above, we first derive the following inequalities; their use is apparent later on:

$$\begin{aligned}
\|\nabla f(X_t)U^*\|_2 &\stackrel{(i)}{\leq} \|\nabla f(X_t)U_t\|_2 + \|\nabla f(X_t)\Delta\|_2 \\
&\stackrel{(ii)}{\leq} \|\nabla f(X_t)U_t\|_2 + \|\nabla f(X_t)Q_\Delta Q_\Delta^\top\|_2 \|\Delta\|_2 \\
&\stackrel{(iii)}{\leq} \|\nabla f(X_t)U_t\|_2 + \left(\|\nabla f(X_t)Q_{U_t}Q_{U_t}^\top\|_2 + \|\nabla f(X_t)Q_{U^*}Q_{U^*}^\top\|_2 \right) \|\Delta\|_2 \\
&\stackrel{(iv)}{\leq} \|\nabla f(X_t)U_t\|_2 + \left(\|\nabla f(X_t)Q_{U_t}Q_{U_t}^\top\|_2 + \|\nabla f(X_t)Q_{U^*}Q_{U^*}^\top\|_2 \right) \frac{1}{200}\sigma_r(U^*) \\
&\stackrel{(v)}{\leq} \|\nabla f(X_t)U_t\|_2 + \frac{1}{(1-\frac{1}{200})} \cdot \frac{1}{200} \|\nabla f(X_t)U_t\|_2 + \frac{1}{200} \|\nabla f(X_t)U^*\|_2 \\
&\leq \frac{200}{199} \|\nabla f(X_t)U_t\|_2 + \frac{1}{200} \|\nabla f(X_t)U^*\|_2.
\end{aligned}$$

where (i) is due to triangle inequality on $U^*R_{U_t}^* = U_t - \Delta$, (ii) is due to generalized Cauchy-Schwarz inequality; we denote as $Q_\Delta Q_\Delta^\top$ the projection matrix on the column span of Δ matrix, (iii) is due to triangle inequality and the fact that the column span of Δ can be decomposed into the column span of U_t and U^* , by construction of Δ , (iv) is due to the assumption $\text{DIST}(U_t, U^*) \leq \rho' \cdot \sigma_r(U^*)$ and

$$\|\Delta\|_2 \leq \text{DIST}(U_t, U^*) \leq \frac{1}{200} \frac{\sigma_r(X^*)}{\sigma_1(X^*)} \cdot \sigma_r(U^*) \leq \frac{1}{200} \cdot \sigma_r(U^*).$$

Finally, (v) is due to the facts:

$$\|\nabla f(X_t)U^*\|_2 = \|\nabla f(X_t)Q_{U^*}Q_{U^*}^\top U^*\|_2 \geq \|\nabla f(X_t)Q_{U^*}Q_{U^*}^\top\|_2 \cdot \sigma_r(U^*),$$

and

$$\begin{aligned}
\|\nabla f(X_t)U_t\|_2 &= \|\nabla f(X_t)Q_{U_t}Q_{U_t}^\top U\|_2 \geq \|\nabla f(X_t)Q_{U_t}Q_{U_t}^\top\|_2 \cdot \sigma_r(U_t) \\
&\geq \|\nabla f(X_t)Q_UQ_U^\top\|_2 \cdot \left(1 - \frac{1}{200}\right) \cdot \sigma_r(U^*),
\end{aligned}$$

by the proof of (a variant of) Lemma A.3 in [8]. Thus, for the term $\|\nabla f(X_t)Q_{U^*}Q_{U^*}^\top\|_2$, we have

$$\begin{aligned}
\|\nabla f(X_t)Q_{U^*}Q_{U^*}^\top\|_2 &\leq \frac{1}{\sigma_r(U^*)} \|\nabla f(X_t)U^*\|_2 \\
&\leq \frac{1}{\sigma_r(U^*)} \frac{201}{199} \|\nabla f(X_t)U_t\|_2 \\
&\leq \frac{201\sigma_1(U^*)}{200\sigma_r(U^*)} \frac{201}{199} \|\nabla f(X_t)Q_{U_t}Q_{U_t}^\top\|_2.
\end{aligned} \tag{29}$$

Using (29) in (28), we obtain:

$$\begin{aligned}
\langle \nabla f(X_t), \Delta\Delta^\top \rangle &\geq - \left(\|\nabla f(X_t)Q_{U_t}Q_{U_t}^\top\|_2 + \frac{201\sigma_1(U^*)}{200\sigma_r(U^*)} \frac{201}{199} \|\nabla f(X_t)Q_{U_t}Q_{U_t}^\top\|_2 \right) \text{DIST}(U_t, U^*)^2 \\
&\geq - \frac{21\cdot\tau(U^*)}{10} \|\nabla f(X_t)Q_{U_t}Q_{U_t}^\top\|_2 \text{DIST}(U_t, U^*)^2
\end{aligned}$$

We remind that the step size we use here is: $\hat{\eta} = \frac{1}{128(L\|X_t\|_2 + \|Q_{U_t}Q_{U_t}^\top \nabla f(X_t)\|_2)}$. Then, we have:

$$\begin{aligned}
&\frac{21\cdot\tau(U^*)}{10} \cdot \|\nabla f(X_t)Q_{U_t}Q_{U_t}^\top\|_2 \cdot \text{DIST}(U_t, U^*)^2 \\
&\leq \frac{21\cdot\tau(U^*)}{10} \cdot \hat{\eta} \cdot 128L\|X_t\|_2 \|Q_{U_t}Q_{U_t}^\top \nabla f(X_t)\|_2 \cdot \text{DIST}(U_t, U^*)^2 \\
&\quad + \frac{21\cdot\tau(U^*)}{10} \cdot \hat{\eta} \cdot 128 \cdot \|Q_{U_t}Q_{U_t}^\top \nabla f(X_t)\|_2^2 \cdot \text{DIST}(U_t, U^*)^2
\end{aligned} \tag{30}$$

To bound the first term on the right hand side, we observe that $\|Q_{U_t} Q_{U_t}^\top \nabla f(X_t)\|_2 \leq \frac{\mu \sigma_r(X_t)}{\frac{21 \cdot \tau(U^*)}{10} \cdot 10}$ or $\|Q_{U_t} Q_{U_t}^\top \nabla f(X_t)\|_2 \geq \frac{\mu \sigma_r(X_t)}{\frac{21 \cdot \tau(U^*)}{10} \cdot 10}$. This results further into:

$$\begin{aligned} & \frac{21 \cdot \tau(U^*)}{10} \cdot \hat{\eta} \cdot 128L\|X_t\|_2 \|Q_{U_t} Q_{U_t}^\top \nabla f(X_t)\|_2 \cdot \text{DIST}(U_t, U^*)^2 \\ & \leq \max \left\{ \frac{\frac{21 \cdot \tau(U^*)}{10} \cdot 128 \cdot \hat{\eta} \cdot L\|X_t\|_2 \cdot \mu \sigma_r(X_t)}{\frac{21 \cdot \tau(U^*)}{10} \cdot 10} \cdot \text{DIST}(U_t, U^*)^2, \right. \\ & \quad \left. \hat{\eta} \left(\frac{21 \cdot \tau(U^*)}{10} \right)^2 \cdot 128 \cdot 10 \kappa \tau(X_t) \|Q_{U_t} Q_{U_t}^\top \nabla f(X_t)\|_2^2 \cdot \text{DIST}(U_t, U^*)^2 \right\} \\ & \leq \frac{128 \cdot \hat{\eta} \cdot L\|X_t\|_2 \cdot \mu \sigma_r(X_t)}{10} \cdot \text{DIST}(U_t, U^*)^2 \\ & \quad + \hat{\eta} \left(\frac{21 \cdot \tau(U^*)}{10} \right)^2 \cdot 128 \cdot 10 \kappa \tau(X_t) \|Q_{U_t} Q_{U_t}^\top \nabla f(X_t)\|_2^2 \cdot \text{DIST}(U_t, U^*)^2, \end{aligned}$$

where $\kappa := \frac{L}{\mu}$ and $\tau(X) := \frac{\sigma_1(X)}{\sigma_r(X)}$ for a rank- r matrix X . Combining the above with (30):

$$\begin{aligned} & \frac{21 \cdot \tau(U^*)}{10} \cdot \|Q_{U_t} Q_{U_t}^\top \nabla f(X_t)\|_2 \cdot \text{DIST}(U_t, U^*)^2 \\ & \stackrel{(i)}{\leq} \frac{\mu \sigma_r(X_t)}{10} \cdot \text{DIST}(U_t, U^*)^2 \\ & \quad + \left(10 \kappa \tau(X_t) \cdot \frac{21 \cdot \tau(U^*)}{10} + 1 \right) \cdot \frac{21 \cdot \tau(U^*)}{10} \cdot 128 \cdot \hat{\eta} \|Q_{U_t} Q_{U_t}^\top \nabla f(X_t)\|_2^2 \cdot \text{DIST}(U_t, U^*)^2 \\ & \stackrel{(ii)}{\leq} \frac{\mu \sigma_r(X_t)}{10} \cdot \text{DIST}(U_t, U^*)^2 \\ & \quad + \left(11 \kappa \tau(X^*) \cdot \frac{21 \cdot \tau(U^*)}{10} + 1 \right) \cdot \frac{21 \cdot \tau(U^*)}{10} \cdot 128 \cdot \hat{\eta} \|Q_{U_t} Q_{U_t}^\top \nabla f(X_t)\|_2^2 \cdot (\rho')^2 \sigma_r(X^*) \\ & \stackrel{(iii)}{\leq} \frac{\mu \sigma_r(X_t)}{10} \cdot \text{DIST}(U_t, U^*)^2 + \frac{12 \cdot 21^2}{10^2} \cdot \kappa \cdot \tau(X^*)^2 \cdot 128 \cdot \hat{\eta} \|\nabla f(X_t) U_t\|_2^2 \cdot \frac{11 \cdot (\rho')^2}{10} \\ & \stackrel{(iv)}{\leq} \frac{\mu \sigma_r(X_t)}{10} \cdot \text{DIST}(U_t, U^*)^2 + \frac{\hat{\eta}}{5} \|\nabla f(X_t) U_t\|_2^2 \end{aligned}$$

where (i) follows from $\hat{\eta} \leq \frac{1}{128L\|X_t\|_2}$, (ii) is due to Lemma A.3 in [8] and using the bound $\text{DIST}(U_t, U^*) \leq \rho' \sigma_r(U^*)$ by the hypothesis of the lemma, (iii) is due to $\sigma_r(X^*) \leq 1.1 \sigma_r(X_t)$ by Lemma A.3 in [8], due to the facts $\sigma_r(X_t) \|Q_{U_t} Q_{U_t}^\top \nabla f(X_t)\|_2^2 \leq \|U_t^\top \nabla f(X_t)\|_F^2$ and $(11 \kappa \tau(X^*) \cdot \frac{21 \cdot \tau(U^*)}{10} + 1) \leq 12 \kappa \tau(X^*) \cdot \frac{21 \cdot \tau(U^*)}{10}$, and $\tau(U^*)^2 = \tau(X^*)$. Finally, (iv) follows from substituting $\rho' := c \cdot \frac{1}{\kappa} \cdot \frac{1}{\tau(X^*)}$ for $c = \frac{1}{200}$ and using Lemma A.3 in [8] (due to the factor $\frac{1}{200}$, all constants above lead to bounding the term with the constant $\frac{1}{5}$).

Thus, we can conclude:

$$\langle \nabla f(X_t), \Delta \Delta^\top \rangle \geq - \left(\frac{\hat{\eta}}{5} \|\nabla f(X_t) U_t\|_F^2 + \frac{\mu \sigma_r(X^*)}{10} \cdot \text{DIST}(U_t, U^*)^2 \right).$$

This completes the proof. \square

7.4 Proof of Corollary 3.2

We have

$$\begin{aligned} \|\tilde{U}_{t+1}\|_F & \leq \|U_t\|_F + \hat{\eta} \cdot \|\nabla f(X_t) U_t\|_F \\ & \leq \|U_t\|_F + \hat{\eta} \cdot \|\nabla f(X_t) Q_{U_t} Q_{U_t}^\top\|_2 \cdot \|U_t\|_F \\ & = (1 + \hat{\eta} \cdot \|\nabla f(X_t) Q_{U_t} Q_{U_t}^\top\|_2) \cdot \lambda \\ & \leq (1 + \frac{1}{128}) \cdot \lambda \end{aligned}$$

where the first inequality follows from the triangle inequality, the second holds by the property $\|AB\|_F \leq \|A\|_2 \cdot \|B\|_F$, and the third follows because the step size is bounded above by $\hat{\eta} \leq \frac{1}{128 \|\nabla f(X_t) Q_{U_t} Q_{U_t}^\top\|_2}$.

Hence, we get $\xi(\tilde{U}_{t+1}) = \frac{\lambda}{\|\tilde{U}_{t+1}\|_F} \geq \frac{128}{129}$.

8 Initialization

In this section, we present a specific initialization strategy for the ProjFGD. For completeness, we repeat the definition of the optimization problem at hand, both in the original space:

$$\underset{X \in \mathbb{R}^{n \times n}}{\text{minimize}} \quad f(X) \quad \text{subject to} \quad X \in \mathcal{C}'. \quad (31)$$

and the factored space:

$$\underset{U \in \mathbb{R}^{n \times r}}{\text{minimize}} \quad f(UU^\top) \quad \text{subject to} \quad U \in \mathcal{C}. \quad (32)$$

For our initialization, we restrict our attention to the full rank ($r = n$) case. Observe that, in this case, \mathcal{C}' is a convex set and includes the full-dimensional PSD cone, as well as other norm constraints, as described in the main text. Let us denote $\Pi_{\mathcal{C}'}(\cdot)$ the corresponding projection step, where all constraints are satisfied simultaneously. Then, the initialization we propose follows similar motions with that in [8]: We consider the projection of the weighted negative gradient at 0, *i.e.*, $-\frac{1}{L} \cdot \nabla f(0)$, onto \mathcal{C}' .¹³ *I.e.*,

$$X_0 = U_0 U_0^\top = \Pi_{\mathcal{C}'}\left(-\frac{1}{L} \cdot \nabla f(0)\right). \quad (33)$$

Assuming a first-oracle model, where we access f only though function evaluations and gradient calculations, (33) provides a cheap way to find an initial point with some approximation guarantees as follows¹⁴:

Lemma 8.1. *Let $U_0 \in \mathbb{R}^{n \times n}$ be such that $X_0 = U_0 U_0^\top = \Pi_{\mathcal{C}'}\left(-\frac{1}{L} \cdot \nabla f(0)\right)$. Consider the problem in (32) where f is assumed to be L -smooth and μ -strongly convex, with optimum point X^* such that $\text{rank}(X^*) = n$. We apply ProjFGD algorithm with U_0 as the initial point. Then, in this generic case, U_0 satisfies:*

$$\text{DIST}(U_0, U^*) \leq \rho' \cdot \sigma_r(U^*),$$

where $\rho' = \sqrt{\frac{1-\mu/L}{2(\sqrt{2}-1)}} \cdot \tau^2(U^*) \cdot \sqrt{\text{srank}(X^*)}$ and $\text{srank}(X) = \frac{\|X\|_F}{\|X\|_2}$.

Proof. To show this, we start with:

$$\|X_0 - X^*\|_F^2 = \|X^*\|_F^2 + \|X_0\|_F^2 - 2 \langle X_0, X^* \rangle. \quad (34)$$

Recall that $X_0 = U_0 U_0^\top = \Pi_{\mathcal{C}'}\left(-\frac{1}{L} \cdot \nabla f(0)\right)$ by assumption, where $\Pi_{\mathcal{C}'}(\cdot)$ is a convex projection. Then, by Lemma 7.1, we get

$$\langle X_0 - X^*, -\frac{1}{L} \cdot \nabla f(0) - X^* \rangle \Rightarrow \langle -\frac{1}{L} \nabla f(0), X^0 - X^* \rangle \geq \langle X^0, X^0 - X^* \rangle. \quad (35)$$

Observe that $0 \in \mathbb{R}^{n \times n}$ is a feasible point, since it is PSD and satisfy any common *symmetric* norm constraints, as the ones considered in this paper. Hence, using strong convexity of f around 0, we get,

$$\begin{aligned} f(X^*) - \frac{\mu}{2} \|X^*\|_F^2 &\geq f(0) + \langle \nabla f(0), X^* \rangle \\ &\stackrel{(i)}{=} f(0) + \langle \nabla f(0), X_0 \rangle + \langle \nabla f(0), X^* - X_0 \rangle \\ &\stackrel{(ii)}{\geq} f(0) + \langle \nabla f(0), X_0 \rangle + \langle L \cdot X_0, X_0 - X^* \rangle. \end{aligned} \quad (36)$$

¹³As in [8], one can approximate easily L , if it is unknown.

¹⁴As we show in the experiments section, a random initialization performs well in practice, without requiring the additional calculations involved in (33). However, a random initialization provides no guarantees whatsoever.

where (i) is by adding and subtracting $\langle \nabla f(0), X_0 \rangle$, and (ii) is due to (35). Further, using the smoothness of f around 0, we get:

$$\begin{aligned} f(X_0) &\leq f(0) + \langle \nabla f(0), X_0 \rangle + \frac{L}{2} \|X_0\|_F^2 \\ &\stackrel{(i)}{\leq} f(X^*) - \frac{\mu}{2} \|X^*\|_F^2 + \langle L \cdot X_0, X^* \rangle - \frac{L}{2} \|X_0\|_F^2 \\ &\leq f(X_0) - \frac{\mu}{2} \|X^*\|_F^2 + \langle L \cdot X_0, X^* \rangle - \frac{L}{2} \|X_0\|_F^2. \end{aligned}$$

where (i) follows from (36) by upper bounding the quantity $f(0) + \langle \nabla f(0), X_0 \rangle$, (ii) follows from the assumption that $f(X^*) \leq f(X_0)$. Hence, rearranging the above terms, we get:

$$\langle X_0, X^* \rangle \geq \frac{1}{2} \|X_0\|_F^2 + \frac{\mu}{2L} \|X^*\|_F^2.$$

Combining the above inequality with (34), we obtain,

$$\|X_0 - X^*\|_F \leq \sqrt{1 - \frac{\mu}{L}} \cdot \|X^*\|_F.$$

Given, U_0 such that $X_0 = U_0 U_0^\top$ and U^* such that $X^* = U^* U^{*\top}$, we use Lemma 7.4 from [44] to obtain:

$$\|U_0 U_0^\top - U^* U^{*\top}\|_F \geq \sqrt{2(\sqrt{2}-1)} \cdot \sigma_r(U^*) \cdot \text{DIST}(U_0, U^*).$$

Thus:

$$\begin{aligned} \text{DIST}(U_0, U^*) &\leq \frac{\|X_0 - X^*\|_F}{\sqrt{2(\sqrt{2}-1)} \cdot \sigma_r(U^*)} \cdot \|X^*\|_F \\ &\leq \rho' \cdot \sigma_r(U^*) \end{aligned}$$

where $\rho' = \sqrt{\frac{1-\mu/L}{2(\sqrt{2}-1)}} \cdot \tau^2(U^*) \cdot \sqrt{\text{srank}(X^*)}$. □

Such initialization, while being simple, introduces further restrictions on the condition number $\tau(X^*)$, and the condition number of function f . Finding such simple initializations with weaker restrictions remains an open problem; however, as shown in [8, 44, 18], one can devise specific deterministic initialization for a given application.

As a final comment, we state the following: In practice, the projection $\Pi_{\mathcal{C}'}(\cdot)$ step might not be easy to compute, due to the joint involvement of convex sets. A practical solution would be to sequentially project $-\frac{1}{L} \cdot \nabla f(0)$ onto the individual constraint sets. Let $\Pi_+(\cdot)$ denote the projection onto the PSD cone. Then, we can consider the approximate point:

$$\tilde{X}_0 = \tilde{U}_0 \tilde{U}_0^\top = \Pi_+(\tilde{X}_0);$$

Given \tilde{U}_0 , we can perform an additional step:

$$U_0 = \Pi_{\mathcal{C}}(\tilde{U}_0),$$

to guarantee that $U_0 \in \mathcal{C}$.